children

*Article*

# Hybrid EEG–EOG Brain–Computer Interface for Virtual-Reality Powered Mobility Training in Children with Severe Neuromotor Disabilities: A Multiple-Case Feasibility Study

**Kevin Marcaccini [1,2,*], Francesca Pulvirenti [2], Francesco Pierotti [3], Laura Dellarole [4], Marzia Bianco [1], Giulia Piermaria [1], Francesca Tampellini [1], Serena Moscato [1,5], Luca Tonin [3,6], Stefano Tortora [3,6], Lorenzo Chiari [1,5], Antonella Cersosimo [2,†] and Silvia Orlandi [1,2,†]**

1 Department of Electrical, Electronic, and Information Engineering "Guglielmo Marconi" (DEI), Alma Mater Studiorum University of Bologna, 40136 Bologna, Italy; mizzi.97@hotmail.it (M.B.); giulia.piermaria3@unibo.it (G.P.); francesca.tampellini99@gmail.com (F.T.); serena.moscato3@unibo.it (S.M.); lorenzo.chiari@unibo.it (L.C.); silvia.orlandi9@unibo.it (S.O.)
2 IRCCS Istituto delle Scienze Neurologiche di Bologna, 40139 Bologna, Italy; francesca.pulvirenti@isnb.it (F.P.); a.cersosimo@isnb.it (A.C.)
3 Department of Information Engineering (DEI), University of Padua, 35131 Padua, Italy; francesco.pierotti@santannapisa.it (F.P.); luca.tonin@unipd.it (L.T.); stefano.tortora@unipd.it (S.T.)
4 Dipartimento Assistenziale Tecnico e Riabilitativo (DATeR) UA Ospedale Maggiore, 40133 Bologna, Italy; laura.dellarole@ausl.bologna.it
5 Health Sciences and Technologies, Interdepartmental Center for Industrial Research (CIRI-SDV), University of Bologna, 40126 Bologna, Italy
6 Padua Neuroscience Center, University of Padua, 35129 Padua, Italy
* Correspondence: kevin.marcaccini@ausl.bologna.it or kevin.marcaccini@unibo.it; Tel.: +39-051-4966403
† These authors contributed equally to this work.

## Highlights

### What are the main findings?

- Four out of six children with severe neuromotor disabilities successfully controlled a virtual reality wheelchair simulator using a hybrid EEG–EOG brain–computer interface, achieving a mean functional accuracy of 77 percent during successful sessions.
- The combined neural interface and virtual reality framework was well-tolerated, demonstrating zero adverse side effects and low user frustration despite the high cognitive demands of kinesthetic motor imagery

### What are the implications of the main findings?

- Combining hybrid neural interfaces with ecologically valid virtual simulators may offer a safe, accessible, and inclusive pathway for powered mobility training in pediatric patients lacking residual motor function.
- The significant performance variability observed in this cohort emphasizes the necessity for personalized calibration strategies and the future integration of semi-autonomous shared control systems before translating this technology to physical wheelchairs.

Check for updates

Academic Editor: Adam Strzelczyk

Received: 9 September 2026
Revised: 30 October 2026
Accepted: 3 November 2026
Published: 5 November 2026

**Copyright:** © 2026 by the authors. Licensee MDPI, Basel, Switzerland. This article is an open access article distributed under the terms and conditions of the Creative Commons Attribution (CC BY) license.

## Abstract

**Background:** Developing Brain–Computer Interfaces (BCIs) for children with severe neuromotor disabilities remains challenging due to developmental neurophysiology and the high cognitive demands of motor imagery. Hybrid BCIs integrating electroencephalography (EEG) and electrooculography (EOG) can overcome these limitations by combining continuous motor-related control with reliable discrete commands. This multiple-case study investigated the feasibility of a hybrid EEG–EOG BCI integrated with a virtual reality (VR) powered wheelchair simulator for mobility training. **Methods**: Six participants (mean age:

13.00 ± 3.52 years; 1 female, 5 males) with severe neuromotor disabilities (i.e., Central Core Myopathy, LAMA2 related Congenital Muscular Dystrophy, Spinal Muscular Atrophy Type II, and Cerebral Palsy) completed repeated sessions using a self-paced BCI. The system combined continuous kinesthetic motor imagery (KMI) for steering and EOG-detected voluntary blinks for discrete commands. We evaluated online classification performance (accuracy, sensitivity, specificity), user workload (NASA-TLX), and simulator-related discomfort (MSAQ) under fully and semi-immersive VR conditions. **Results**: Across the selected session-level evaluations, mean online classification accuracy was 67%, increasing to 77% when considering only successful evaluations. Four of the six participants completed the experimental protocol, whereas two discontinued after T3 because sufficiently stable BCI control could not be achieved. NASA-TLX scores indicated increasing perceived workload but generally low frustration, while low MSAQ scores suggested good VR tolerability. No participants withdrew because of VR-related discomfort or adverse effects. **Conclusions**: This exploratory study provides preliminary evidence supporting the feasibility of hybrid EEG–EOG BCI control within a VR-based powered mobility simulator for children and adolescents with severe neuromotor disabilities. Although simulated navigation was feasible for four participants, substantial variability in BCI control highlights the need for further technological refinement and validation in larger cohorts.

**Keywords:** brain computer interface; kinesthetic motor imagery; virtual reality; neuromotor disabilities; powered mobility

## 1. Introduction

Independent mobility is a fundamental prerequisite for cognitive, social, and emotional development in children [1]. For children with severe neuromotor disabilities, powered wheelchairs (PWs) can provide an important means of achieving independent mobility and promoting autonomous exploration and participation in daily life. However, conventional PWs typically require residual upper-limb function for their operation, which may be limited or absent in this population [2]. It is indeed estimated that up to 10–15% of potential PW users are unable to operate standard joystick-based interfaces due to profound motor impairments [3,4]. While powered mobility (PM) systems remain the primary assistive technologies to improve functional independence and, consequently, health-related quality of life [5], this physical barrier creates a critical accessibility gap during crucial developmental stages.

Even for users capable of alternative access, safe and effective PW use requires specific driving skills. Conventionally, wheelchair training (WT) is delivered in structured clinical settings under direct therapist supervision. Although this approach ensures patient safety and standardized skill acquisition, often guided by pediatric frameworks like the Powered Mobility Program (PMP) [6], it places considerable demands on clinical resources, specialized personnel, and infrastructure [7]. Technology-assisted and home-based solutions may complement conventional training by increasing opportunities for individualized, repeated practice outside clinical settings.

Virtual reality (VR) has emerged as a promising platform for mobility training, providing safe, controlled, and repeatable environments for skill acquisition [8]. Both fully immersive (FI) systems, using head-mounted displays, and semi-immersive (SI) desktop configurations can simulate ecologically meaningful driving scenarios while removing the physical risks of real-world practice [7]. Furthermore, VR enables minimally supervised, high-intensity sessions that are highly suitable for home-based WT [9].

Despite these advantages, existing VR wheelchair training simulators often fail to bridge the aforementioned accessibility gap for users with severe upper-limb dysfunction [10]. Many systems lack realistic driving challenges and, most importantly, do not support interoperability with alternative, joystick-free control interfaces [11,12]. The development of reliable alternative access strategies is therefore essential to ensure VR-mediated PM training is truly inclusive.

Brain–computer interfaces (BCIs) offer a viable solution by enabling users to control external devices through physiological signals, bypassing neuromuscular pathways [13]. While BCIs have been increasingly investigated as assistive technologies [14,15] and integrated with VR environments [16], transitioning them from laboratory prototypes to practical clinical tools remains hindered by variable performance, demanding training, and high user burden [17].

These challenges are exceptionally pronounced in pediatric BCI research. Pediatric BCIs represent a particularly challenging and clinically relevant research domain. Recent clinical evidence further supports the growing interest in pediatric BCI applications, highlighting their potential as assistive technologies while emphasizing the need for developmentally appropriate protocols and clinically meaningful outcome measures [18]. A systematic review by Orlandi et al. highlighted that pediatric BCI studies are still predominantly feasibility-oriented, characterized by small sample sizes and high performance variability [19]. Pediatric users present unique challenges, including higher inter- and intra-subject variability, shorter attention spans, susceptibility to fatigue, and ongoing neurodevelopmental changes [19–21]. Nevertheless, clinical studies demonstrate that children with severe neurological disabilities can achieve functional BCI control, provided that calibration and training procedures are highly individualized and user-centered [22,23].

Among non-invasive BCI paradigms, motor imagery (MI)-based approaches are particularly suited for mobility applications. Unlike stimulus-driven paradigms (e.g., P300 or SSVEP), MI enables endogenous, continuous, and self-paced control without relying on external sensory stimulation [24,25]. Specifically, kinesthetic motor imagery (KMI), the internal reproduction of proprioceptive and somatosensory sensations associated with movement [26], is strongly linked to sensorimotor activation, making it a highly effective directional control strategy [27,28]. Although KMI is cognitively demanding and can induce fatigue [19,29], engaging residual sensorimotor networks actively exploits the high neuroplastic potential typical of childhood [30–32]. Previous evidence confirms that pediatric users can perform KMI and achieve functional control, albeit with greater variability than adults [20–23].

To address these cognitive demands and improve overall reliability, hybrid BCIs combine neural signals with additional physiological inputs. Integrating electroencephalography (EEG) with electrooculography (EOG) to detect voluntary eye blinks provides complementary control channels that enhance decoding robustness and command separability [13,33,34]. This multimodal strategy is especially relevant in pediatric contexts, where EEG signal variability can severely limit single-modality control [35]. Recent studies support this direction, showing that multimodal paradigms enhance engagement [20,22] and that children can achieve meaningful functional mobility outcomes even with variable classification performance [36].

Despite these advancements, a significant literature gap remains. Current pediatric BCI research focuses heavily on communication tasks or simplified laboratory interfaces, while existing VR simulators remain largely joystick-dependent. Although recent clinical evidence has demonstrated the feasibility of BCI-enabled powered mobility training in children [36], the integration of a hybrid EEG-EOG control framework within an immersive VR-based wheelchair training protocol has not yet been investigated.

In response to these gaps, we developed BCI4VR-PMP, a hybrid EEG-EOG platform integrating self-paced KMI control with a VR-powered wheelchair simulator. This multiple-case feasibility study evaluated BCI-related online controllability, usability, and workload, along with VR tolerability in children and adolescents with severe neuromotor disabilities.

## 2. Materials and Methods

### *2.1. Study Design*

This exploratory multiple-case feasibility study was designed to evaluate the accessibility, online controllability, usability, and tolerability of a hybrid EEG-EOG BCI integrated with a VR-powered wheelchair simulator in children and adolescents with severe neuromotor disabilities. Owing to the rarity and heterogeneity of the target population, a multiple-case design was selected instead of a conventional group-comparison design. Participants were recruited from the "UOC Medicina Riabilitativa Infantile (UOC-MRI)" unit of the IRCCS Institute of Neurological Sciences of Bologna (IRCCS-ISNB). Experiments were performed after prior informed consent and under the supervision of physicians, neurologists, or physiotherapists. The study was conducted in accordance with the ethical principles established by the Declaration of Helsinki and was approved by the local Ethical Committee (37-2023-OSS-AUSLBO). The protocol is registered on ClinicalTrials.gov (ID: NCT06586125) and is part of a broader research project investigating the integration of VR and BCIs. Specifically, this manuscript presents the findings related to the BCI component.

### *2.2. Participant Recruitment*

Participant recruitment was done according to the following inclusion criteria:

1. Both genders.
2. Ages between 6 and 20 years.
3. PMP score higher than 0.
4. Clinical diagnosis of severe neuromotor disability associated with substantial limitations in independent mobility. The mobility-related descriptions of Gross Motor Function Classification System (GMFCS [37]) levels III–V were used as a descriptive reference to characterize functional mobility limitations, including in participants with diagnoses other than cerebral palsy. However, the GMFCS was not considered a formally validated classification instrument for neuromuscular disorders.
5. Use of either a PW or a manual wheelchair with an electric propulsion system.

Based on these criteria, six participants without prior experience with VR or BCI technologies were enrolled (mean age: 13.00 ± 3.52 years; 1 female, 5 males). The inclusion criteria regarding age (6 to 20 years) and the absence of sex restrictions were intentionally maintained broad to align with the exploratory feasibility nature of this study. Given the rarity of severe neuromotor disabilities requiring powered mobility interventions, enforcing narrower demographic restrictions would have rendered the recruitment process at the clinical center excessively prolonged or practically impossible. Indeed, the limited sample size reflects the practical complexities of conducting multiple experimental sessions with severely impaired pediatric patients who require continuous caregiver support. Participants were intentionally selected to represent the spectrum of pediatric neuromotor disorders commonly requiring powered mobility, while preserving sufficient cognitive abilities to perform the demanding KMI and VR tasks. Detailed demographic and clinical characteristics are reported in Table 1. The absence of cognitive impairments was established through formal evaluations conducted by the referring pediatric neuropsychiatrists. Cognitive functioning was assessed using age appropriate standardized psychometric instruments, specifically the Wechsler Intelligence Scale for Children Fourth Edition (WISC IV) and the

Wechsler Preschool and Primary Scale of Intelligence Third Edition (WPPSI III). Based on the available clinical neuropsychological assessments, participants were considered to have sufficient cognitive abilities to understand and follow the experimental instructions. This determination was made by the referring clinical team and was used to establish eligibility for the BCI protocol. Furthermore, none of the participants presented perceptual disorders or epilepsy. Regarding visual conditions, BCI03 had mild myopia, and BCI06 had astigmatism. All participants had previous experience operating powered wheelchairs. While a formal baseline assessment of their physical driving skills was not conducted prior to enrollment, the duration of their prior powered mobility experience was documented based on their first prescription dates. Specifically, the years of first prescription were 2019 for BCI01, 2014 for BCI02, 2017 for BCI03, 2021 for BCI04, 2020 for BCI05, and 2024 for BCI06. Because the experimental tests were conducted between 2024 and 2025, this confirms that the majority of the cohort had several years of daily driving experience prior to the BCI intervention. Ongoing pharmacological therapies were reported only for BCI04 and BCI06, who were under respiratory bronchodilator and salbutamol therapy, respectively.

The recruited participants presented heterogeneous patterns of residual motor function, reflecting the clinical variability of the target population. Lower-limb (LL) motor control was severely impaired in all participants, with only BCI01 retaining limited voluntary ankle movement, whereas the remaining participants exhibited minimal motor control confined to the hip region. Upper-limb (UL) function showed greater variability, ranging from residual proximal arm movements (e.g., elbow flexion or forearm pronation/supination) to isolated finger movements. Detailed information on residual UL and LL motor abilities for each participant is reported in Table 1.

**Table 1.** Participants' information.

| ID | Age | Sex | Disorder | Residual UL Motor Function | Residual LL Motor Function |
|---|---|---|---|---|---|
| BCI01 | 14 | F | Central Core Myopathy | Forearm pronation/supination | Limited ankle movement |
| BCI02 | 13 | M | LAMA2-related Congenital Muscular Dystrophy (MDC1A) | Elbow flexion | Minimal motor control at hip |
| BCI03 | 18 | M | SMA II | Elbow flexion | Minimal motor control at hip |
| BCI04 | 13 | M | SMA II | Index finger dorsiflexion | Minimal motor control at hip |
| BCI05 | 13 | M | CP | Proximal UL, hand, and finger | Minimal motor control at hip |
| BCI06 | 7 | M | SMA II | Proximal UL, hand, and finger | Minimal motor control at hip |

BCI—Brain Computer Interface, CP—Cerebral Palsy, F—Female, ID—Identifier, LAMA2—Laminin Subunit Alpha 2, LL—Lower Limb, M—Male, MDC1A—Muscular Dystrophy Congenital Type 1A, SMA II—Spinal Muscular Atrophy Type II, UL—Upper Limb.

Participants with residual motor function were intentionally included, consistent with the exploratory feasibility nature of this study. Residual motor experience is considered advantageous for KMI, as this paradigm relies on the internal representation of previously experienced movements and their associated proprioceptive sensations [38]. Conversely, the complete or congenital absence of voluntary motor function may limit the development of accurate motor representations and potentially reduce KMI performance. Future studies

will extend the evaluation of the proposed framework to participants with more severe motor impairments.

### *2.3. BCI4VR-PMP System*

The system used in this study, the BCI4VR-PMP (depicted in Figure 1a) consists of two integrated modules: a VR wheelchair-driving simulator (VR-PMP, depicted in Figure 1c) and a hybrid EOG-EEG BCI system.

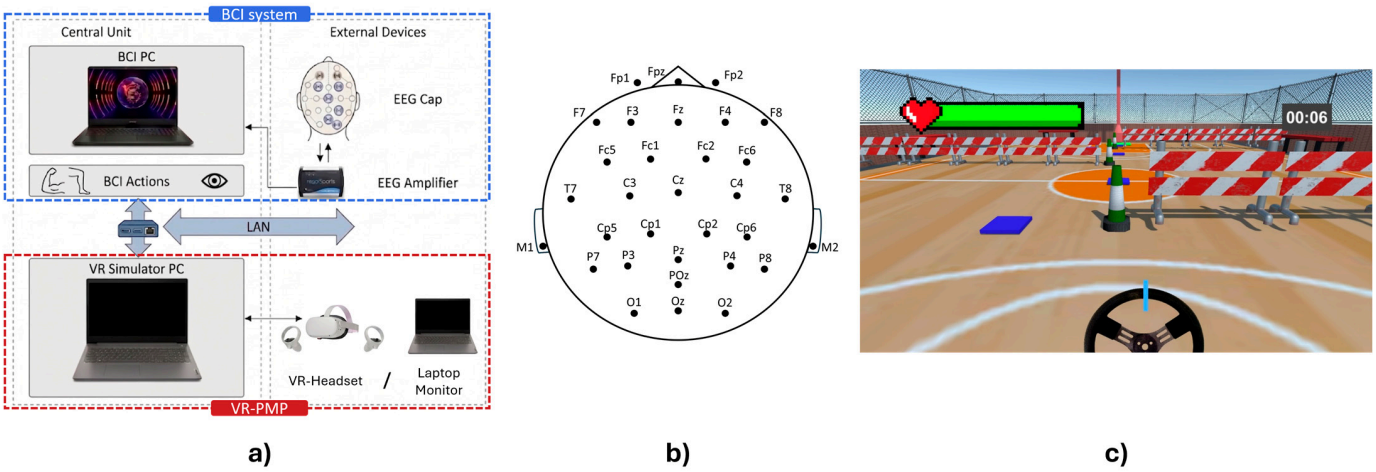



**Figure 1.** (**a**) System Description; (**b**) EEG montage; (**c**) Task 12 VR-PMP Example.

EEG recordings were acquired through a 32-channel Waveguard cap (EEG64-BIP24CA209, ANT Neuro, Hengelo, The Netherlands) arranged according to the international 10–20 layout (depicted in Figure 1b). The cap was connected to an eego Sports amplifier (ANT Neuro, Hengelo, The Netherlands), and signals were digitized at a sampling frequency of 512 Hz. Additionally, ocular activity was monitored by thresholding the deflections of frontal electrodes, specifically Fp1 and Fp2.

The VR-PMP simulator was developed using Unity (Unity Technologies, San Francisco, CA, USA) and designed to simulate the first 20 tasks of the PMP in both FI and SI VR environments.

The hybrid BCI system was developed within the ROS-Neuro framework [39]. Signal pre-processing included the application of a Common Average Reference (CAR) spatial filter to implement average re-referencing across all channels. The power spectral density was computed via Welch's algorithm using a 1 s Hamming window sliding every 62.5 ms, yielding an update frequency of 16 Hz. Following feature selection via Canonical Variate Analysis (CVA), continuous classification was performed using a Gaussian classifier. The classifier parameters were initialized via self-organizing maps clustering and trained using a gradient descent-based supervised learning algorithm. During online control, posterior probabilities were accumulated using a leaky integrator based on exponential smoothing. A steering command was generated immediately once the integrated probability reached the activation threshold, with no additional fixed dwell time required. For the EOG-based discrete commands, signals from the frontal electrodes (Fp1 and Fp2) were mirrored in the time domain and band pass filtered from 1 to 10 Hz using a second order Butterworth filter. An amplitude threshold was applied to detect intentional blinks, immediately followed by an empirically validated 1 s refractory period to prevent accidental double triggers from subsequent spontaneous eye movements.

The VR simulator and the BCI module run on two dedicated computers connected via a TCP/IP LAN connection, enabling seamless real-time control of the virtual environment through the physiological data.

The hybrid BCI can discriminate between three specific classes to drive the virtual wheelchair. Specifically, imagining the movement of the UL rotates the wheelchair by 30 degrees to the left, while imagining the movement of the lower limbs LL rotates it by 30 degrees to the right. Finally, discrete voluntary eye blinks are used to intentionally start and stop the forward motion of the wheelchair at a fixed speed.

More detailed technical information about the system can be found in a previous work [40] in which we tested it on a group of six participants without disabilities, demonstrating the feasibility and usability on that court.

### *2.4. Experimental Protocol*

The experimental protocol is illustrated in Figure 2a. It consists of a clinical assessment (Tca), a preliminary session (Tprel), and three to four experimental sessions (T1–T4), with at least 3 days between consecutive time points.

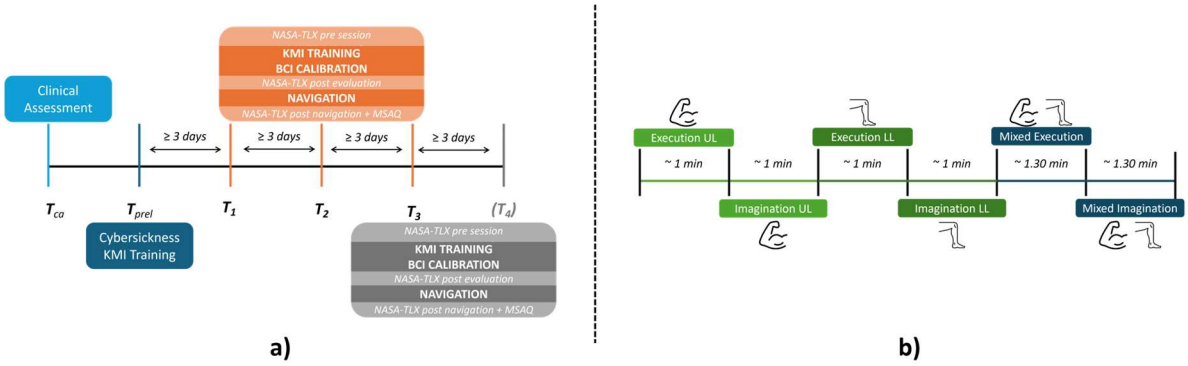



**Figure 2.** (**a**) Acquisition protocol scheme; (**b**) KMI training protocol (BCI: brain computer interface; KMI: Kinesthetic Motor Imagery; LL: Lower Limbs; MSAQ: motion sickness assessment questionnaire; NASA-TLX: NASA task load index; UL: Upper Limbs).

### *2.5. Preliminary Session*

Once the movements were chosen, the next preliminary phase (Tprel) started, the same day as Tca. In the beginning, cybersickness, a known adverse effect associated with VR exposure [41], was tested on a dedicated assessment module of the VR-PMP simulator. To this aim, participants were instructed to navigate two distinct virtual environments (a park and a city scenario) for a cumulative duration of 8 min. The simulator modality was then selected according to predefined age and VR-tolerability criteria. In compliance with VR headset usage guidelines [42,43], participants younger than 13 years old were restricted to the SI version of the VR-PMP simulator due to safety concerns and the potential for adverse effects. For participants aged 13 years or older, the presence or absence of VR-related side effects observed during the preliminary assessment was used to determine the most appropriate simulator modality (FI or SI).

To assess cybersickness, the motion sickness assessment questionnaire (MSAQ) [44] was used. Although the Simulator Sickness Questionnaire (SSQ) [45] is commonly employed to assess symptoms associated with VR exposure, the MSAQ provides a broader multidimensional characterization of motion sickness symptoms, encompassing gastrointestinal, central, peripheral, and sopite-related manifestations. Moreover, previous research using the MSAQ showed that cybersickness and classical motion sickness are characterized by largely comparable symptom profiles [41]. The MSAQ has also been previously used to

assess visually induced motion sickness in VR-based wheelchair simulators [46], further supporting its use in the present study. Importantly, cybersickness monitoring was not limited to questionnaire administration. At each session, participants were explicitly asked about discomfort and modality preferences, with the possibility to switch VR modality, when necessary, in order to minimize adverse effects and prevent study withdrawal.

Afterwards, each participant underwent the KMI training (KMIT). This training had two aims. Primarily, it provided standardized training on the KMI paradigm adopted for BCI calibration and control. Additionally, it was systematically administered at the beginning of each of the subsequent sessions to orient participants' attention toward the target movements before EEG acquisition and BCI operation. As illustrated in Figure 3b, the KMIT protocol began with 1 min of motor execution of the specific UL movement decided for each participant, followed by a corresponding KMI of the same movement. Both the execution and imagery blocks consisted of 10 consecutive trials, each comprising a few seconds of active task followed by a brief rest. The same sequence was then performed for LL movements. The protocol concluded with a mixed condition in which participants responded to visual cues by alternately executing and imagining UL and LL movements presented in randomized order (seven trials per effector). The mixed block had a total duration of approximately 90 s. The duration of each block was intentionally kept short to ensure focused engagement and to minimize cognitive and physical fatigue, given the overall length of the experimental sessions and the pediatric clinical population involved.

To guide participants through the KMI training, visual cues corresponding to the target movements and preparation intervals were presented on a laptop screen, as shown in Figure 3.

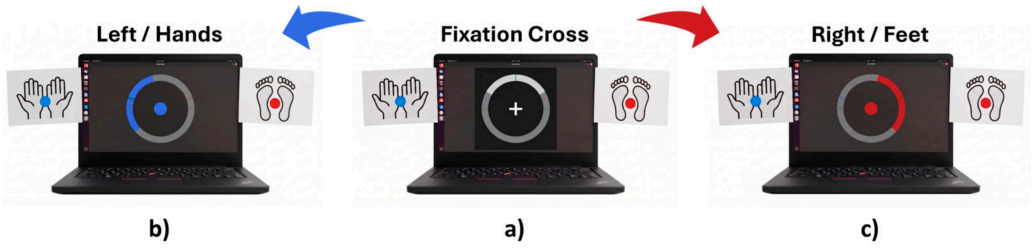



**Figure 3.** KMIT Feedback: (**a**) Hands MI or ME feedback; (**b**) Fixation cross feedback; (**c**) Feet MI or ME feedback.

These specific visual cues were selected to ensure consistency with the subsequent BCI calibration procedure, detailed in the following section. To further support the cognitive association between the target movement, the visual cue, and the resulting wheelchair direction, visual aids depicting hands and feet were attached to the sides of the laptop monitor. This setup was specifically designed to help pediatric participants internalize the control strategy and minimize cognitive load.

Crucially, these visual aids were kept physically attached to the monitor throughout the later BCI calibration, evaluation, and VR navigation phases. This strategy aimed to continuously help the children in recalling the correct imagery-to-command associations without increasing memory burden.

The previous literature on motor imagery training suggests that shorter, repeated blocks may help preserve imagery quality and attentional resources, especially in rehabilitation settings [47–49]. Participants were instructed to continue KMIT at home for a minimum of three days between each experimental sessions. To support them during this independent practice, participants were provided with video recordings, replicating the exact visual cues and timing used in the laboratory setting. This was meant to ensure consistent guidance and reinforcing the correct imagery-to-command associations during the execution of

the home-based KMIT. However, it must be noted that while home practice was strongly recommended, compliance was not objectively monitored through digital logs or diaries. Participants were simply asked, during the ambulatory sessions, if they had performed the KMIT in the previous days or not.

Conversely, no specific preliminary training was conducted for the eye-blinking command. Prior to calibration, each participant's ability to voluntarily and reliably produce eye blinks was assessed and confirmed. Given the adequate voluntary control observed in all participants, individual calibration of the EOG detection threshold during the session was considered sufficient to ensure reliable system operation.

### *2.6. Experimental Sessions*

After a minimum interval of three days, participants attended the first experimental session (T1), starting with the repetition of the KMIT. The structure and progression of all experimental BCI sessions (T1–T4) are summarized in Table 2.

**Table 2.** Structure of BCI experimental sessions.

| Session | Calibration (Training) | Evaluation | VR Navigation |
|---|---|---|---|
| T1 | Yes | Yes | Preview (5 levels) |
| T2 | If needed | Yes | Full (20 levels) |
| T3 | If needed | Yes | Full (20 levels) |
| T4 | If needed | Yes | Full (20 levels) |

VR–Virtual Reality.

Subsequently, the BCI classifier was trained for each participant by acquiring at least three runs, each composed of ten repetitions of UL and ten of LL KMI, presented randomly through visual cues, as described by the article of Tonin et al. [50]. Then, the online accuracy of each participant with the system was tested through the evaluation session, in which participants performed in random order 20 trials (10 UL, 10 LL), with the aim of reaching a predefined activation threshold. A session was considered successful if classification accuracy exceeded 60% (see Marcaccini et al. [40] for the detailed methodology), and it could have been repeated twice. In the case of a successful evaluation phase, the threshold for detection of eye blinking was individually calibrated. Participants were instructed to perform voluntary blinks while different values were tested, aiming to identify the optimal threshold that reliably discriminated intentional blinks from involuntary ones. To ensure system reliability before proceeding, the selected threshold was definitively confirmed only if the participant successfully triggered the command with five consecutive voluntary blinks, without eliciting any false positives during spontaneous blinking. A higher number of trials was deliberately avoided to prevent unnecessary physical and visual fatigue prior to the main navigation task, taking into consideration the young age and clinical conditions of the participants. Subsequently, participants used the BCI system to navigate through 5 of the 20 levels of the VR-PMP in order to provide a preview of the tasks they would have to perform in the next sessions. Full navigation across all VR-PMP levels was intentionally avoided since, given the relatively young age of the population, the session duration was intentionally kept as short as possible.

Later sessions (T2–4) were separated by at least three days to allow continued at-home KMIT. These sessions followed the same general structure as T1 with minor adaptations. Specifically, the evaluation stage was performed immediately after KMIT, using the classifier trained during T1. Recalibration was carried out only if performance during evaluation was considered insufficient, followed by a repeated evaluation. Upon completion of the final

system evaluation, participants proceeded to the VR-BCI Navigation phase, during which they completed all 20 tasks of the VR-PMP simulator by controlling the virtual wheelchair via BCI.

Session T4 was optional and scheduled only when adequate BCI control was not achieved in T2 or T3. Study discontinuation would have occurred if reliable BCI control was not obtained in more than one session among T2, T3, and T4. Failure at T1 was considered acceptable, given the expected adaptation challenges during first exposure in pediatric and adolescent participants.

Perceived workload was assessed in all BCI sessions using the NASA Task Load Index (NASA-TLX) questionnaire [51], administered in three different time-points: before the session (pre-session, PS), after system evaluation (post-evaluation, PE), and when participants had control of the system, after the navigation phase (post-navigation, PN). The evaluation of potential VR-related side effects was performed after the navigation phase, using the MSAQ.

### 2.7. Data Analysis

To evaluate the feasibility of the proposed system within this multiple-case design, study outcomes were divided into primary and secondary measures. Primary outcomes focused on online controllability and BCI performance metrics, including online accuracy, sensitivity, and specificity. Secondary outcomes encompassed system usability and patient tolerability, evaluated through the NASA-TLX workload index, MSAQ side effects, drop-outs, user tolerance, and adherence to the protocol.

### 2.8. BCI Performance

BCI performance was quantified during the evaluation phase of each session. For every session, classification outcomes were summarized in a confusion matrix, from which overall accuracy and class-specific metrics were derived. Correct identification of UL imagery trials was defined as the positive class (true positive, TP), whereas correct LL imagery trials were defined as the negative class (true negative, TN). Misclassifications were limited to incorrect activation of the non-target class, corresponding to false positives (FP) or false negatives (FN). Trials in which the instructed class did not reach any activation threshold were not considered classification errors and were therefore excluded from FP and FN counts. This definition was selected because failure to activate the classifier resulted in no directional command rather than an unsafe movement, as initiation and termination of wheelchair movement were controlled independently via voluntary eye blinks. This choice reflects the operational logic of the system, in which the KMI paradigm was used to steer the virtual wheelchair left or right. An incorrect class activation would have resulted in steering in the unintended direction, being a potentially unsafe event. In contrast, failure to reach the activation threshold resulted in no directional command, which did not pose safety concerns. Based on this framework, sensitivity reflected the proportion of correctly detected UL imagery trials, while specificity represented the correct identification of LL imagery trials.

It is worth noting that formal classification metrics were not computed for the EOG-based voluntary blink commands.

### 2.9. VR Navigation Performance

Task completion times and collision counts were extracted to characterize navigation performance within the virtual environment. Since the virtual environment is a custom-built platform, contextualizing these values required a standardized baseline. To this aim, reference recordings were obtained from an experienced adult laboratory member

(26 years old, female) under two conditions: BCI-based control and conventional manual control. These recordings were used as exploratory reference values rather than as normative benchmarks or estimates of theoretical maximum performance.

### *2.10. System Usability*

Subjective workload was assessed using the NASA-TLX, computed according to the original scoring procedure [51]. Percentual scores were obtained for each of the six fields (mental demand, physical demand, temporal demand, performance, effort, and frustration), and the overall workload index was calculated. In addition to the raw scores collected at each assessment point, delta values were computed to quantify changes between PS and PE, and between PE and PN. NASA-TLX workload scores were collected across three assessment phases: PS, PE, and PN. Given the small sample size of participants who completed the full protocol (i.e., 4 individuals), participants completed repeated sessions across the study.

Due to the small sample size and the feasibility nature of the study, subjective workload data derived from the NASA TLX questionnaire were evaluated using purely descriptive statistics rather than inferential hypothesis testing. Data distributions are reported using medians, interquartile ranges, and absolute minimum to maximum ranges to represent the data spread without risking inferential overreach. To assess phase dependent workload changes, differential scores comparing the workload increases generated by the calibration phase and the virtual reality navigation phase were visually evaluated using boxplots.

### *2.11. VR-Related Side Effects*

The evaluation of potential VR-related side effects was performed using the MSAQ. In accordance with Gianaros et al. [44], four subscales (gastrointestinal, central, peripheral, and drowsiness) as well as the total score were computed and expressed as percentage values. Comparisons across sessions (Tprel, T1, T2, T3 and T4) and stimulation modalities (SI and FI) were explored descriptively through graphical representations. Inferential statistical analyses were not conducted due to the extremely limited sample size and the structural characteristics of the dataset. Specifically, only four participants completed all sessions with sufficient BCI control, yielding four repeated observations per time point. In addition, the number of sessions conducted with the FI modality ($n = 6$) was markedly lower than those performed with the SI modality ($n = 13$), resulting in an unbalanced design. Importantly, the choice of stimulation modality was not randomized but driven by individual clinical needs and practical constraints, introducing potential confounding factors that would not be adequately controlled in a formal statistical comparison.

All computations were implemented in MATLAB (R2025b).

## 3. Results

### *3.1. Feasibility and Protocol Adherence*

Four out of six participants (67%) successfully completed the protocol, whereas two participants (BCI01 and BCI06) did not achieve stable online control and discontinued the study after T3, in accordance with predefined protocol cut offs. Moreover, only one participant (BCI004) required session T4. The overall study progression, including enrollment and session completion, is summarized in Figure 4.

Furthermore, regarding the independent training protocol, all participants verbally reported adherence to the recommended at-home KMI practice when queried at the beginning of each clinical session.

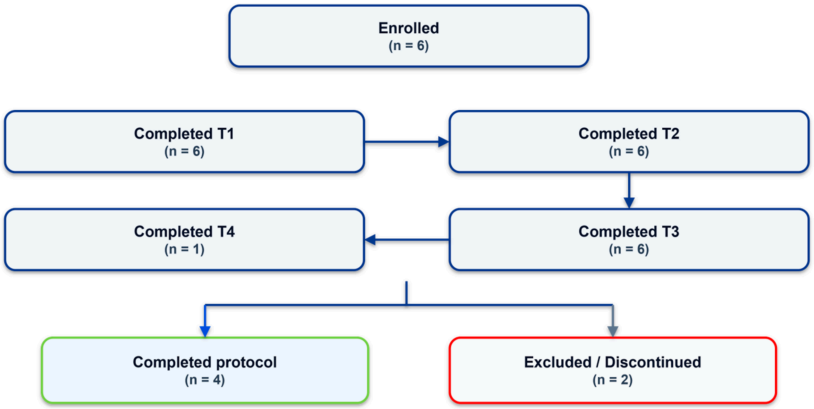



**Figure 4.** Study progression and protocol adherence.

### *3.2. Individualized KMI Task Selection*

As a result of the clinical evaluation session, specific UL and LL movements were selected for each participant based on their residual motor abilities. The LL movement was standardized as hip adduction–abduction for almost all participants, with the exception of BCI01 who performed feet dorsiflexion. Conversely, UL movements were highly individualized: hand opening-closing for BCI05 and BCI06; bicep curl for BCI03; elbow flexion–extension with a pronated forearm supported on the wheelchair tray for BCI02; stabilized forearm pronation–supination for BCI01; and gravity-assisted index finger flexion–extension for BCI04.

### *3.3. Navigation Eligibility and Recalibration*

Participants BCI02, BCI03, BCI04, and BCI05 achieved sufficient accuracy in at least two sessions among T2, T3, and T4; therefore, they were eligible to perform the corresponding full navigation phases and successfully completed the protocol. Regarding system recalibration, all participants required it during session T2. In session T3, recalibration was necessary for participants BCI01, BCI04, and BCI05, while BCI04 required it during the optional session T4.

### *3.4. Features and Thresholds*

Table 3 summarizes the EEG used to train the classifier and the corresponding threshold values.

The feature columns report, for each participant and session, the combination of EEG channels (in bold) and the associated frequencies (in Hz, indicated in round brackets), used to extract the power spectral density as input features for the BCI. Specifically, these features were selected by identifying the most discriminative ones between the two KMI classes using a Canonical Variate Analysis. The table also reports the thresholds used for the recognition of UL and LL KMI, as well as the thresholds for voluntary blink detection expressed in microvolts ($\mu V$). When a threshold was modified during the navigation session, the most recent value is reported in round brackets, whereas the value outside the brackets corresponds to the one used during the BCI calibration and evaluation phases. Given the deterministic nature of the thresholding approach and the inherently high signal-to-noise ratio of ocular artifacts, the blink detection proved to be highly reliable. All participants successfully used the blink command to intentionally initiate and terminate the wheelchair movement without reported operational issues during the sessions.

**Table 3.** Selected features and thresholds in sessions T1–T4.

| ID | T1 | | T2 | | T3 | | T4 | |
|---|---|---|---|---|---|---|---|---|
| | **Features** | **Thresholds** | **Features** | **Thresholds** | **Features** | **Thresholds** | **Features** | **Thresholds** |
| BCI01 | C3 (8, 14 Hz) | UL: 0.56<br>LL: 0.56<br>EOG: 100 uV | FC1 (12 Hz), FC5 (14 Hz) | UL: 0.56<br>LL: 0.56<br>EOG: 100 uV | FC1 (16 Hz), CP1 (14 Hz), CP6 (16 Hz) | UL: 0.52<br>LL: 0.77 | | |
| BCI02 | FC5 (16 Hz), FC2 (16 Hz), FC1 (18 Hz) | UL: 0.59<br>LL: 0.54<br>EOG: 200 uV | C3 (10, 12 Hz) | UL: 0.68 (0.61)<br>LL: 0.64<br>EOG: 120 uV | C3 (10, 12 Hz) | UL: 0,63<br>LL: 0,63<br>EOG: 125 uV | | |
| BCI03 | C3 (12 Hz), C4 (16 Hz), CP6 (20 Hz) | UL: 0.58<br>LL: 0.55<br>EOG: 120 uV | C3 (12 Hz), CP1 (12 Hz) | UL: 0.55<br>LL:0.53<br>EOG: 125 uV | C3 (12 Hz), CP1 (12 Hz) | UL: 0.55<br>LL: 0.58<br>EOG: 125 uV | | |
| BCI04 | CP5 (10, 12 Hz), C3 (10, 12 Hz) | UL: 0,60<br>LL:0.57<br>EOG: 125 uV | C4 (10, 16, 18 Hz), CP5 (10 Hz) | UL: 0.60<br>LL: 0.65 (0.60)<br>EOG: 125 uV | CZ (16 Hz), CP2 (16 Hz) | UL: 0.59<br>LL: 0.54 | C4 (10, 12 Hz), CP6 (12 Hz) | UL: 0.59<br>LL: 0.55<br>EOG: 125 uV |
| BCI05 | FC2 (16 Hz), FC6 (16, 18 Hz) | UL: 0.56<br>LL: 0.62 | FC5 (14 Hz), FC2 (16 Hz), C4 (12 Hz) | UL: 0.77<br>LL: 0.53<br>EOG: 121 uV | FC5 (14 Hz), FC2 (16 Hz), C4 (12 Hz) | UL: 0.60<br>LL: 0.55<br>EOG: 121 uV | | |
| BCI06 | FC5 (18 Hz), FC2 (18 Hz), CZ (10 Hz) | UL: 0.62<br>LL: 0.63 | C3 (26,28 Hz), CP2 (26,28 Hz) | UL: 0.58<br>LL: 0.63 | C4 (10, 12 Hz) | UL: 0.60<br>LL: 0.63 | | |

C—central; CP—Centro-parietal; ID—identifier; EOG—electrooculography; F—frontal; FC—fronto-central; LL—lower limbs; UL—upper limbs.

### *3.5. Classification Metrics*

Table 4 summarizes the classification performance obtained in each session. When participants performed multiple evaluations within the same session (i.e., in case of failed evaluation sessions), only the evaluation with the highest accuracy was retained to characterize the best performance achieved following calibration or recalibration. This approach was consistent with the operational objective of determining whether participants could proceed to VR navigation. However, selecting the highest-performing evaluation may provide an optimistic estimate of sustained BCI performance, and the reported session-level metrics should therefore not be interpreted as averages across all evaluation attempts.

**Table 4.** Evaluation phase no-decision rate, raw accuracy, sensitivity, and specificity scores.

| ID | Session | No-Decision Rate | Accuracy | Sensitivity | Specificity |
|---|---|---|---|---|---|
| BCI01 | T1 | 0.45 | **0.70** | 0.40 | 1.00 |
| | T2 | 0.25 | 0.53 | 0.00 | 1.00 |
| | T3 | 0.00 | 0.50 | 0.00 | 1.00 |
| BCI02 | T1 | 0.05 | 0.52 | 0.40 | 0.67 |
| | T2 | 0.40 | **1.00** | 1.00 | 1.00 |
| | T3 | 0.35 | **0.85** | 1.00 | 0.60 |
| BCI03 | T1 | 0.40 | **0.92** | 0.86 | 1.00 |
| | T2 | 0.25 | **0.67** | 0.86 | 0.50 |
| | T3 | 0.20 | **0.69** | 0.89 | 0.43 |
| BCI04 | T1 | 0.20 | **0.62** | 0.29 | 0.89 |
| | T2 | 0.30 | **0.71** | 0.78 | 0.60 |
| | T3 | 0.15 | 0.41 | 0.71 | 0.20 |
| | T4 | 0.30 | **0.79** | 1.00 | 0.50 |
| BCI05 | T1 | 0.15 | 0.53 | 0.67 | 0.38 |
| | T2 | 0.25 | **0.93** | 0.88 | 1.00 |
| | T3 | 0.60 | **0.62** | 0.40 | 1.00 |
| BCI06 | T1 | 0.35 | **0.77** | 0.40 | 1.00 |
| | T2 | 0.25 | 0.53 | 1.00 | 0.12 |
| | T3 | 0.30 | 0.50 | 0.83 | 0.25 |

Bold values represent sufficient (i.e., ≥0.60) accuracies. (ID—Identifier).

Across all evaluation sessions and participants, mean online accuracy was 0.67 ± 0.16 (mean ± standard deviation, SD), with a sensitivity of 0.65 ± 0.32 (mean ± SD) and a specificity of 0.69 ± 0.31. When evaluating the temporal progression across the protocol, the overall mean online accuracy and SD values were 0.68 ± 0.15 at T1, 0.73 ± 0.20 at T2, and 0.60 ± 0.15 at T3.

Considering only successful sessions (i.e., the ones with accuracy ≥ 60%), mean online accuracy increased to 0.77 ± 0.12, alongside a sensitivity of 0.87 ± 0.11 and a specificity of 0.90 ± 0.16. Finally, when isolating the subgroup of four participants who successfully completed the entire protocol, the mean online accuracy trends across the sessions were 0.65 ± 0.19 in T1, 0.83 ± 0.16 in T2, and 0.64 ± 0.18 in T3.

As defined by the protocol, a session was considered successful and proceeded to the navigation phase if the classification accuracy exceeded the a priori functional threshold of 60%, a standard benchmark for effective BCI control [52,53]. Across the control periods that met this criterion, the mean online classification accuracy was 77%. This value is descriptive,

and no formal inferential test against chance was performed. Therefore, the 60% threshold should be interpreted as an operational criterion for proceeding to navigation, rather than as evidence of statistically significant above-chance classification.

To fully characterize the system's responsiveness for real-world application, we also evaluated the frequency of trials in which no command was produced (i.e., the KMI classifier did not reach the activation threshold for either class), calling this parameter the no-decision rate. Consistent with the accuracy metrics, this rate was extracted exclusively from the best evaluation run of each session. Across all evaluation sessions, the mean 'no-decision' rate was 27.37 ± 13.98%. When considering only the successful sessions (accuracy ≥ 60%), the mean rate of unclassified trials was 33.75 ± 11.51%.

A formal accuracy value for the EOG-based eye-blinking command was not computed. During calibration, participants were required to achieve five consecutive successful voluntary activation without false-positive detection before proceeding to the VR navigation phase. Accordingly, all participants who advanced to the VR navigation phase had already demonstrated highly reliable control over the blinking command.

### *3.6. VR Navigation Performance*

Figure 5 presents the mean completion times and number of collisions for the four successful participants, compared against reference values from the expert user with and without BCI control.

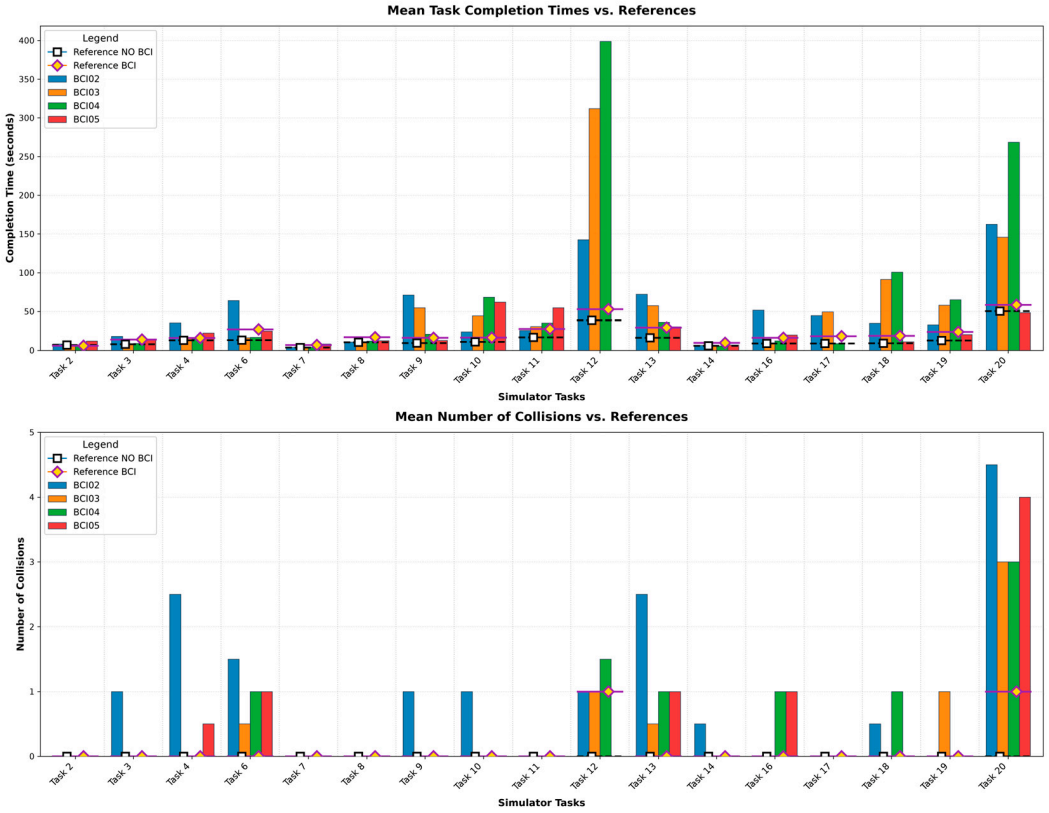



**Figure 5.** Quantitative behavioral metrics for VR navigation. The (**top panel**) displays the mean task completion times in seconds for each participant across the simulator tasks, compared to reference BCI and non-BCI control values. The (**bottom panel**) displays the mean number of collisions per task.

### *3.7. System Usability*

For consistency, descriptive analyses were performed only on sessions in which participants completed the calibration, evaluation, and navigation timepoints, yielding all NASA-TLX values (i.e., PS, PE, and PN). For this reason, the following sessions were ex-

cluded: BCI01 sessions T2 and T3, BCI02 session T1, BCI04 session T3, BCI05 session T1, and BCI06 session T2 and T3.

The distribution of NASA-TLX mental demand and overall scores across participants and BCI sessions (PS, PE, and PN) is reported in Figure 6a,b. Mental demand was specifically highlighted as the proposed task is primarily cognitive.

To provide an overview, Table 5 reports the median and the ranges for all NASA-TLX subscales, calculated across the sessions and divided into timepoints. Figure 6c,d present the differential workload scores used to visually compare the relative demands of the calibration and navigation phases. The plotted values represent the absolute changes in NASA TLX scores between the assessment intervals: Pre Session to Post Evaluation, and Post Evaluation to Post Navigation.

**Table 5.** NASA-TLX median scores across timepoints.

| | Pre Session | Post Evaluation | Post Navigation |
|---|---|---|---|
| Total Score | Median: 36.66<br>IQR: 23.33 to 48.00<br>Range: 8.33 to 66.00 | Median: 56.16<br>IQR: 45.33 to 66.33<br>Range: 11.67 to 75.67 | Median: 69.50<br>IQR: 59.67 to 78.33<br>Range: 25.67 to 86.00 |
| Mental Demand | Median: 35.00<br>IQR: 0.00 to 50.00<br>Range: 0.00 to 65.00 | Median: 67.50<br>IQR: 55.00 to 80.00<br>Range: 0.00 to 85.00 | Median: 85.00<br>IQR: 65.00 to 85.00<br>Range: 45.00 to 95.00 |
| Physical Demand | Median: 20.00<br>IQR: 0.00 to 25.00<br>Range: 0.00 to 45.00 | Median: 30.00<br>IQR: 10.00 to 45.00<br>Range: 0.00 to 55.00 | Median: 42.50<br>IQR: 20.00 to 45.00<br>Range: 0.00 to 60.00 |
| Temporal Demand | Median: 10.00<br>IQR: 0.00 to 15.00<br>Range: 0.00 to 45.00 | Median: 22.50<br>IQR: 5.00 to 35.00<br>Range: 0.00 to 55.00 | Median: 30.00<br>IQR: 20.00 to 55.00<br>Range: 0.00 to 60.00 |
| Performance | Median: 50.00<br>IQR: 30.00 to 70.00<br>Range: 25.00 to 85.00 | Median: 52.50<br>IQR: 45.00 to 65.00<br>Range: 35.00 to 90.00 | Median: 72.50<br>IQR: 65.00 to 85.00<br>Range: 40.00 to 100.00 |
| Effort | Median: 25.00<br>IQR: 5.00 to 35.00<br>Range: 0.00 to 65.00 | Median: 60.00<br>IQR: 30.00 to 70.00<br>Range: 0.00 to 85.00 | Median: 70.00<br>IQR: 45.00 to 85.00<br>Range: 0.00 to 100.00 |
| Frustration | Median: 2.50<br>IQR: 0.00 to 10.00<br>Range: 0.00 to 45.00 | Median: 2.50<br>IQR: 0.00 to 30.00<br>Range: 0.00 to 60.00 | Median: 22.50<br>IQR: 0.00 to 45.00<br>Range: 0.00 to 65.00 |

Values are reported as Median, interquartile ranges (IQR) and range percentage scores across all fully completed sessions.

Consistent with the rationale described above, both the mental demand and the overall workload differential scores are shown.

As detailed in Table 5, descriptive NASA-TLX results suggested an increase in perceived workload across the assessment points, particularly in mental demand and effort. The median overall Total Score increased from a baseline of 36.66 before the session to 56.16 after the evaluation phase, ultimately reaching 69.50 following the continuous navigation task. The median Mental Demand score instead increased from 35.00 prior to the session to 67.50 after the evaluation, peaking at 85.00 after virtual navigation. Effort and Performance dimensions followed similar increasing trends. Conversely, Frustration remained generally low throughout the core BCI interaction, maintaining a median floor value of 2.50 through the evaluation phase and rising to 22.50 after navigation.

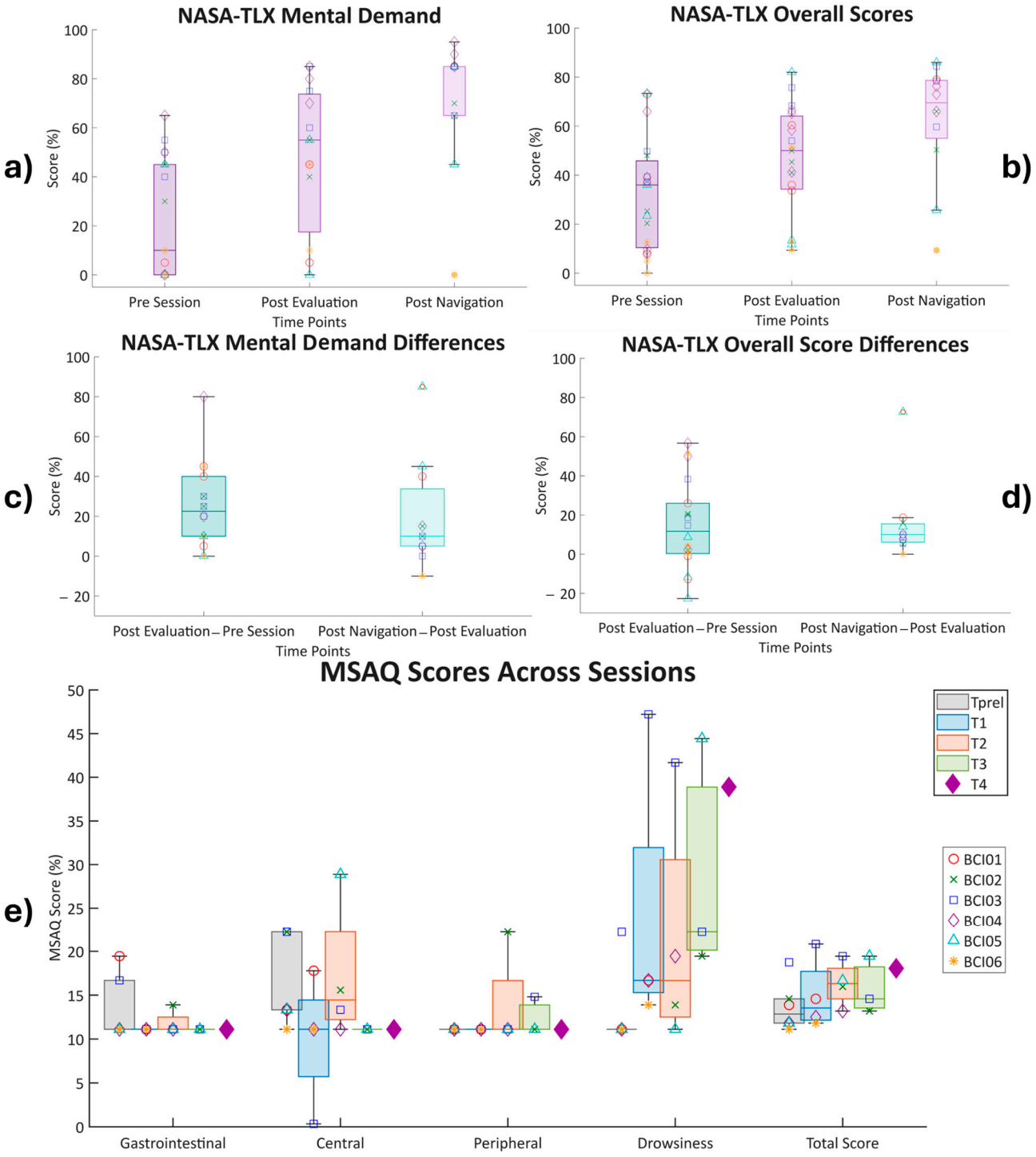



**Figure 6.** (**a**) Distribution of NASA-TLX mental demand scores across all sessions, expressed as percentage values. (**b**) Distribution of NASA-TLX total scores across all sessions, expressed as percentage values. (**c**) Distribution of the delta values between the three time points for the NASA-TLX mental demand scores, expressed as percentage values. (**d**) Distribution of the delta values between the three time points for the NASA-TLX total scores, expressed as percentage values. (**e**) MSAQ scores across sessions for the different extracted subscales. Session T4 includes data from a single participant (i.e., BCI04).

Regarding the differential score analysis, visual inspection of the delta values indicates that both the calibration phase and the navigation phase contributed to the cognitive burden in similar magnitude.

However, substantial variability was observed across participants and sessions. Given the small number of independent participants, these patterns should be interpreted descriptively rather than as evidence of statistically significant changes.

### *3.8. Virtual Reality Modality and Tolerability*

Regarding the VR modalities used across the experimental protocol, participants BCI05 and BCI06 used the SI setup exclusively. For BCI06, this choice was dictated by age-related restrictions associated with VR headset use, whereas for BCI05 the SI modality was selected a priori because of severe visual impairment and involuntary head movements, which could have been exacerbated by the weight and visual demands of the headset. The remaining participants initially used the FI modality but transitioned to the SI setup during the protocol to improve comfort: BCI03 and BCI04 switched from T2 onwards, while BCI01 and BCI02 transitioned during T3. Reasons for FI-to-SI change are reported for each participant in the next section.

As illustrated by Figure 6e, the MSAQ total scores remained below 20% across all sessions and modalities.

### *3.9. Individual Case Studies*

To address the inter-subject variability, individual clinical profiles and performance trajectories are summarized in Table 6 and detailed below.

**Table 6.** Individual participant findings.

| Participant | Main Findings |
|---|---|
| BCI01 | Persistently insufficient control |
| BCI02 | Rapid learning effect and high accuracy |
| BCI03 | Early and stable proficiency |
| BCI04 | Control achieved through extended training |
| BCI05 | Variable but functional performance |
| BCI06 | Progressive performance instability (age-related) |

BCI01 was a 14-year-old female with central core myopathy presenting minimal residual motor control (limited ankle movement and forearm pronation/supination). In session T1, classification accuracy reached 0.70, with a sensitivity of 0.40. In subsequent sessions (T2 and T3), performance declined to accuracies of 0.53 and 0.50, respectively, and a sensitivity of 0.00. The participant transitioned from the FI to the SI modality in T3. Overall, she tolerated the VR environment without significant side effects, but the inability to reach consistent control thresholds led to her exclusion after T3.

BCI02 was a 13-year-old male diagnosed with LAMA2-related congenital muscular dystrophy (MDC1A), presenting residual elbow motor control and minimal lower-limb function. Following an unsuccessful evaluation in T1 (accuracy = 0.52), online performance substantially improved, reaching perfect classification accuracy in T2 (accuracy = 1.00; sensitivity = 1.00; specificity = 1.00). Performance remained above the predefined success threshold (i.e., 60%) in T3 (accuracy = 0.85), allowing successful completion of all navigation sessions. The participant initially used the FI VR modality but switched to the SI configuration from T3 onward because of discomfort related to the brightness of the head-mounted display.

BCI03 was an 18-year-old male with SMA II, presenting mild myopia, minimal hip control, and residual elbow motor control. The participant achieved an accuracy of 0.92

in T1. In subsequent sessions, accuracies decreased but remained sufficient for control (0.67 in T2; 0.69 in T3). During T1, BCI03 reported an MSAQ total score of 20.83% and an overall NASA-TLX score increase of 38.34 between PS and PE. The participant switched from FI to SI VR from T2 onward due to pre-existing cervical musculoskeletal limitations. BCI03 maintained reliable functional control and completed the experimental protocol successfully.

BCI04 was a 13-year-old male with SMA II, presenting severe UL impairment (restricted to index finger dorsiflexion) and minimal hip control. The participant required the maximum number of sessions (T1-T4) to complete the protocol due to an insufficient T3. Accuracy values were 0.62 in T1 and 0.71 in T2, dropping to 0.41 in T3, before recovering to 0.79 in T4. System recalibration was necessary in T3 and T4. BCI04 switched from FI to SI modality starting in T2, reporting pronounced fatigue related to the VR headset. During sessions T1 and T2, the participant exhibited increases between PS and PE in NASA-TLX mental demand (approximately 80%) and overall workload (between 50% and 60%). The participant successfully completed the protocol.

BCI05 was a 13-year-old male with CP who retained residual finger, hand, and proximal UL motor abilities. Due to severe visual impairment and involuntary head movements, this participant used the SI modality exclusively throughout the protocol. After an accuracy of 0.53 in T1, performance peaked at 0.93 in T2, but fell to 0.62 in T3, necessitating recalibration. The participant achieved the required thresholds in T2 and T3, successfully completing the protocol without notable VR-related side effects. Substantial increases in NASA-TLX scores were observed between the PE and PN time points in session T3, with delta values reaching approximately 85% for mental demand and 72% for overall workload.

BCI06 was a 7-year-old male with SMA II who retained residual finger, hand, and proximal UL motor control. Due to age restrictions associated with head-mounted display usage guidelines, the participant utilized the SI modality exclusively. He achieved functional control in T1 (accuracy = 0.77) but failed subsequent sessions, scoring 0.53 in T2 and 0.50 in T3. While sensitivity was high in later sessions (1.00 in T2; 0.83 in T3), specificity dropped drastically (0.12 in T2; 0.25 in T3). Consequently, the participant was excluded after T3.

Overall, no participant reported serious adverse events related to either the BCI system or the VR environment, and no withdrawals occurred because of cybersickness.

## 4. Discussion

The present multiple-case feasibility study demonstrated that most participants achieved functional online control of the proposed hybrid EEG–EOG BCI while maintaining good tolerability and minimal VR-related adverse effects. Although classification performance was characterized by substantial inter-subject variability, the observed online accuracies were consistent with previous pediatric MI-based BCI studies [54–56]. Indeed, the primary objective of a mobility-oriented BCI is not maximizing classification accuracy per se, but enabling safe, interpretable, and functional interaction with the environment.

From a clinical feasibility perspective, our system prioritized accessibility and usability. Four out of the six enrolled participants effectively completed the protocol, demonstrating reliable controllability of the virtual wheelchair. When considering the classification metrics, it is essential to analyze both the overall baseline performance and the performance during successful control periods. Across all conducted evaluations, the system achieved a mean overall accuracy of approximately 67%. This metric is highly representative of the inherent day-to-day variability and the significant challenges encountered when deploying MI-based BCIs in a pediatric clinical setting, capturing the instances where fatigue, attention deficits, or suboptimal calibration temporarily hindered control. However, despite these fluctuations, when participants were able to surpass the minimal control threshold, the

mean accuracy reached 77%. Both the overall 67% baseline and the 77% peak functional performance must be contextualized within the clinical and developmental characteristics of the population under investigation. Pediatric BCI studies have consistently reported performance values typically ranging between 60% and 80% [20,21]. As highlighted by a systematic review focusing on pediatric BCI applications, performance variability and training requirements represent key limiting factors in this demographic [19]. For these reasons, in clinical pediatric settings, accuracy values around or above 70% are generally considered indicative of effective and functional BCI control [23].

Comparable findings have been reported in studies targeting BCI-based powered mobility. For instance, Hammond et al. [36] showed that nine pediatric users achieved functional control despite high BCI calibration variability. While they evaluated physical wheelchairs using commercial EEG systems in real-world settings, our study utilized a custom hybrid EEG–EOG framework within a VR simulator prior to physical exposure. Despite these methodological differences, both studies converge on a critical conclusion: variable classification accuracy does not prevent pediatric users from acquiring functional BCI control. Similarly, Floreani et al. [22] reported that children with severe motor disabilities successfully engaged with BCI systems at performance levels comparable to those seen in the present study. When compared to controlled or non-clinical MI studies, the observed performance appears lower but stays clinically meaningful. A substantial part of the literature reports classification accuracies above 80% or 90% derived from offline analyses on public datasets, often involving neurotypical participants [24]. However, such values do not reflect real-time interaction. In contrast, real-time BCI applications involving mobility control commonly report performance in the 60–85% range, supporting the validity of the present online evaluations.

For a more direct comparison, an earlier study evaluating the same BCI system in neurotypical adults reported a mean online accuracy and SD of 71 ± 21% [40]. The comparable performance achieved by the pediatric clinical cohort in the present study shows that no specific modifications to the calibration procedure or classifier configuration were needed to accommodate potential neurophysiological differences [57]. Notably, unlike the earlier study [40] where sensitivity was disproportionately higher than specificity, the present results show a more balanced relationship between the two metrics. This symmetric detection of the two KMI classes shows a more stable classification behavior, which is critical for reliability in practical BCI mobility applications.

Furthermore, the evaluation of trials where no command was produced provides important context for real-world usability. The observed no-decision rates highlight an important trade-off between directional classification reliability and command availability. Although conservative activation thresholds may reduce unintended directional commands, failure to generate a command can impair navigation responsiveness. In particular, maintaining the current trajectory may not always be safe when approaching obstacles or performing complex maneuvers. Therefore, both incorrect activations and command omissions should be considered when evaluating the functional reliability and potential safety of the system.

### *4.1. Hybrid EEG–EOG Control and KMI Training*

A key innovative aspect of the present work lies in the integration of KMIT, hybrid EEG–EOG control, and a structured VR-based WT paradigm. While many pediatric BCI systems rely on stimulus-driven paradigms, such as the P300, due to their robustness [58], these approaches are typically limited to discrete and exogenous interactions. In contrast, KMI-based paradigms enable endogenous, continuous, and self-paced control, which is strictly needed for realistic navigation tasks [24]. However, MI-based approaches are intrinsically more demanding and less stable, particularly in pediatric populations [19].

To mitigate these challenges, the hybrid integration with EOG signals enhances system robustness by introducing complementary control channels, reducing classification ambiguity, and overall improving usability. Hybrid BCIs have been shown to improve reliability in complex interaction scenarios [13]. In the present study, the effectiveness of this approach was confirmed by the participants' subjective experience. Specifically for the EOG-based eye blinking control, none of the participants reported any difficulty in executing the voluntary eye-blinking commands during the VR navigation, suggesting that the control strategy was well-tolerated and functionally adequate for the navigation task. Furthermore, the implementation of a structured KMI training protocol, supported by the continuous visual aids (i.e., the virtual steering wheel providing directional feedback, alongside the images of hands and feet displayed on the screen sides), represents an additional strength. Guided motor imagery training has been shown to improve performance and engagement, particularly in rehabilitation settings [47], and proved to be highly beneficial in supporting the specific cognitive demands of the pediatric participants in this study.

### *4.2. Inter-Subject Variability*

The substantial inter-individual variability observed in this study may reflect differences in age, clinical diagnosis, residual motor abilities, motor imagery strategies, and participant-specific neurophysiological characteristics. However, the small and heterogeneous sample does not allow the independent contribution of these factors to be determined. Accordingly, these potential associations should be interpreted as hypotheses for future investigation rather than as established explanations of individual BCI performance.

A key finding of the present study is the marked inter-subject variability in BCI performance. While some participants rapidly achieved stable control (ranging up to 100% accuracy), others struggled to reach consistent activation thresholds. This variability is a defining characteristic of MI-based BCIs, and it is heavily amplified in pediatric populations due to interconnected clinical and neurodevelopmental factors [21].

The relationship between motor impairment and KMI abilities warrants particular consideration. In children with CP, a systematic review found moderate evidence of similar imagery vividness compared with typically developing peers, although evidence concerning the capacity to generate motor imagery and its temporal correspondence with actual movement remained inconclusive [59]. In a small EEG study, children with CP demonstrated cortical activation during KMI involving the sensorimotor, premotor, and supplementary motor areas, although their activation patterns differed from those of typically developing children [60]. Moreover, a BCI study involving 14 individuals with CP found that eight participants achieved statistically significant online control with at least one of two tested BCI paradigms, including six who controlled a sensorimotor-rhythm-based BCI [61]. Together, these findings indicate that CP does not necessarily preclude motor-imagery-related cortical activity or BCI control, although the ability to generate usable control signals varies across individuals.

Relevant evidence is also available for neuromuscular disorders, although studies involving children with the specific diagnoses represented in our cohort remain limited. Georgiadis et al. investigated motor-imagery-based EEG decoding in six adults with neuromuscular disorders, including spinal muscular atrophy and different muscular dystrophies. They reported altered functional connectivity patterns and showed that phase-synchrony features could support individualized decoding of imagined left- versus right-hand movements [62]. In a separate single-case study, an adult with severe muscular dystrophy controlled a virtual avatar through motor imagery of the feet and hands. Following five months of training, the EEG classification error rate decreased from 40% to 28% [63]. These studies support the feasibility of motor-imagery-based BCI control in individuals with sub-

stantial neuromuscular impairment. However, their adult samples, different classification tasks, and distinct signal-processing and training procedures preclude direct comparison with the mean online accuracy observed in the present study.

Motor imagery should nevertheless not be assumed to remain unaffected by neuromuscular disease. In a study of children with Duchenne muscular dystrophy, scores on validated motor-imagery questionnaires were lower than those of healthy controls [64]. Although Duchenne muscular dystrophy was not represented in our cohort, this finding suggests that motor-imagery ability may vary in neuromuscular populations. Severe motor impairment should therefore not be treated as either evidence of preserved imagery or proof of imagery failure. The relationship may depend on the specific condition and individual characteristics, as well as on the method used to assess imagery. Evidence from related disorders cannot, however, establish how motor imagery is affected specifically in spinal muscular atrophy type II, LAMA2-related congenital muscular dystrophy, or central core myopathy.

In the present cohort, initial difficulty achieving reliable control did not necessarily preclude subsequent functional use. The individual trajectories suggest that training and recalibration may help some participants establish or recover effective control, although the present sample does not allow us to determine which clinical or neurophysiological factors explain these changes [22,23,65]. Indeed, while all participants required system recalibration in T2, only one needed it in later sessions.

Furthermore, neurodevelopmental heterogeneity and fatigue play crucial roles in these performance fluctuations. Maintaining sustained attention for repetitive KMI tasks is particularly challenging for very young pediatric users, where cognitive fatigue can lead to a sudden drop in performance across sessions despite an initially successful calibration.

This need for individualization was also reflected in the clinical choice of the target KMI tasks. A greater task variability was seen for UL movements compared to LL ones, reflecting both the broader inclusion criteria for UL residual function and the intrinsically higher degrees of freedom of UL articulations. Nevertheless, this task heterogeneity is unlikely to have affected the classification outcomes. Current literature indicates that standard EEG-based techniques struggle to discriminate different MI tasks within the same limb [56,66], suggesting that simple differences between imagined UL movements were less relevant for the classifier than the macroscopic spatial distinction between the UL and LL classes.

The validity of the classification process is further supported by the feature selection outcomes. For all participants, the selected channels consistently localized over the sensorimotor cortex, and the identified frequency components (8–28 Hz) overlapped perfectly with classical alpha (8–12 Hz) and beta (12–30 Hz) rhythms. This is consistent with the well-established role of these cortical areas and oscillatory activities in voluntary motor planning and execution [67,68]. Interestingly, these spatial and spectral features closely mirror those selected in our earlier work with neurotypical individuals using the exact same system. While the present feasibility study cannot draw firm conclusions on neurophysiological differences between populations, this similarity shows that the neural patterns exploited by the classifier remained robust and comparable despite the presence of severe neuromotor disabilities.

### *4.3. VR Navigation Performance*

Beyond successful command classification, the kinematic outcomes demonstrated that the four participants who achieved sufficient BCI control could use the hybrid framework to navigate the virtual environment and complete all 20 tasks. Performance was generally comparable to the BCI reference values, particularly during basic navigation, stopping, and simple turning maneuvers. However, Task 12, involving a continuous zigzag slalom

around cones, and Task 20, requiring multiple consecutive left and right turns, resulted in the longest completion times and highest collision rates. These findings highlight the limitations of the current KMI-based control strategy when handling complex maneuvers that require frequent and sustained switching between upper limb and lower limb motor imagery. Such transitions may increase cognitive demands and contribute to delayed or missed directional commands, potentially explaining the reduced performance observed in these tasks. Nevertheless, successful completion of the entire task set indicates that the proposed hybrid framework can support functional powered mobility within a simulated environment, although further improvements are needed to enhance the precision and reliability of complex maneuvers.

### *4.4. Usability, Workload, and Engagement*

Beyond classification accuracy, the present study contributes important insights into system usability, specifically regarding the interplay between cognitive workload, user frustration, and task engagement.

The NASA-TLX results indicated moderate-to-high overall workload levels, with evident increases across sessions primarily driven by the mental demand and effort sub-scales. This trend is consistent with earlier findings showing that MI-based BCI control is inherently cognitively demanding [69]. In pediatric populations, this cognitive fatigue is a critical factor influencing both performance and compliance, as demonstrated by Keough et al. [29]. Notably, the differential workload scores between the calibration and navigation phases did not show relevant differences. This contrasts with the adult neurotypical group evaluated in our previous work [40], where VR navigation was found to be significantly less demanding than standard calibration.

Despite this high cognitive burden, the reported frustration remained low compared to the other workload dimensions. As detailed in Table 6, the median frustration score maintained a floor value of 2.50 during the baseline and evaluation phases, before rising modestly to 22.50 following the continuous virtual navigation. While this represents a visible descriptive increase induced by the complex steering tasks, this peak value remains substantially lower than the primary cognitive drivers such as mental demand. This overall low frustration profile, coupled with the absence of dropouts related to task intolerance, suggests that the system was well-tolerated by the participants even when physical navigation proved challenging.

Anyway, even if these observations indicate acceptable task tolerability among participants who completed the protocol, they do not establish a causal relationship between VR engagement, workload, and perceived performance.

Crucially, this tolerance can be explained by a high level of engagement. Scores in the NASA-TLX performance sub-scale, which reflects perceived success, showed a clear upward descriptive trend across the assessment phases, reaching a median of 72.50 after the navigation task. This suggests that the goal-oriented VR interaction successfully fostered a strong feeling of achievement and motivation, effectively compensating for the high mental demand and mitigating frustration.

The evaluation of VR-related side effects further supports this feasibility. As measured by the MSAQ, minimal negative effects were seen. Interestingly, participants did not switch VR modality because of cybersickness. Instead, the 4 transitions made by participants BCI01-BCI04 were motivated by comfort, fatigue, musculoskeletal limitations, or hardware-related factors. This suggests that prolonged VR use is feasible even in pediatric neuromotor populations when the stimulation modality is individualized. The integration of VR stands as a key contribution of the present study, enabling the implementation of ecologically valid training scenarios. VR is widely recognized as an effective tool for skill acquisition in

rehabilitation [70], and its combination with BCI systems may enhance accessibility and motivation for users with severe motor impairments.

### *4.5. Limitations*

Despite these promising findings, several limitations should be acknowledged. First, the small sample size limits generalizability, although this is consistent with a feasibility-oriented design and the inherent challenges of recruiting a pediatric clinical population requiring caregiver support. Second, participant clinical heterogeneity and unavoidable variability in session scheduling, primarily driven by real-world logistical constraints, may have influenced learning effects and fatigue levels. In addition, while all participants self-reported high adherence to the independent at-home KMI training between sessions, this compliance was not objectively monitored through digital logs or telemetry. Because self-reported data is susceptible to recall bias or overestimation, the observed session-to-session performance fluctuations cannot be definitively separated from actual differences in training volume, cognitive fatigue, or classifier recalibration effects.

Moreover, while the EOG-based blink command was validated prior to navigation, we did not quantitatively record missed or unwanted blinks during the actual VR driving task. Gathering these data would have required constantly probing the participants regarding their real-time movement intentions, which would have limited the ecological validity of the simulation and may have artificially increased frustration. Consequently, online command reliability during navigation was inferred from qualitative observation and participant task completion rather than quantitative trial-by-trial metrics.

Although the number and duration of experimental sessions were intentionally limited to reduce participant burden, this design restricted the assessment of long-term BCI learning and performance stability.

From a technical and methodological perspective, the reliance on conventional gel-based EEG systems, which require time-consuming preparation, may limit the scalability and daily applicability of the setup. In addition, the absence of a comparator condition (e.g., joystick control or a non-hybrid BCI) prevents direct quantification of the added value provided by the hybrid architecture.

Finally, although all participants were habitual powered wheelchair users, a formal standardized assessment of their physical driving skills was not performed prior to the study. Consequently, the extent to which their varying degrees of pre-existing wheelchair proficiency influenced their virtual navigation success remains unquantified, representing an additional limitation when interpreting the behavioral metrics.

### *4.6. Future Work*

To address these limitations and move toward clinical translation, future work should focus on expanding the cohort through multicenter studies. This will be necessary to validate the findings on a larger scale, particularly including individuals with more severe or congenital motor disabilities.

From a hardware and usability standpoint, the adoption of more user-friendly technologies, such as dry or semi-dry EEG sensors, will be crucial to reduce setup times and facilitate the potential home deployment of the system.

Moreover, future protocols should incorporate a higher number of sessions to assess long-term learning effects. This longitudinal approach, combined with detailed neurophysiological analyses comparing neural patterns between successful and unsuccessful users, will inform the development of robust, adaptive decoders capable of continuous personalized classification.

Translating these VR-based findings into physical environments by testing the framework on a real wheelchair, alongside the systematic integration of safety metrics and functional outcome measures, will be the ultimate step to confirm clinical efficacy. Furthermore, deploying this technology in a physical environment will fundamentally require the integration of the BCI with shared control approaches and semi-autonomous navigation systems [71–74]. As demonstrated by the recent literature, embedding intelligent robotic assistance to share the steering burden and prevent environmental collisions is essential to guarantee user safety and ensure effective daily mobility. Finally, as pediatric BCI technologies move closer to daily applications, evaluating the impact of different VR modalities (e.g., SI versus FI) and addressing ethical and regulatory considerations, particularly regarding future invasive and implantable solutions, will become increasingly important [75].

## 5. Conclusions

This exploratory multiple-case study provides preliminary evidence supporting the feasibility of integrating a hybrid EEG–EOG BCI with a VR-based powered mobility simulator for children and adolescents with severe neuromotor disabilities. Four of the six participants completed the experimental protocol, while substantial inter-individual variability and difficulties in achieving stable BCI control were observed. Although the VR environment was generally well-tolerated and participants who achieved sufficient BCI control completed simulated navigation tasks, the findings do not establish improvements in powered mobility skills or safety in real-world wheelchair operation. Further studies are needed to improve command reliability, optimize individualized training strategies, and validate functional navigation outcomes.

Unlike many laboratory BCI studies, the present framework was specifically designed around an existing clinical assessment (i.e., PMP), increasing its potential for integration into pediatric rehabilitation pathways. The possibility of combining standardized wheelchair training with hybrid BCI control may facilitate future implementation in rehabilitation centers and, eventually, home-based training programs.

**Author Contributions:** Conceptualization, K.M., A.C. and S.O.; methodology, K.M., S.O., F.P. (Francesco Pierotti), F.T. and G.P.; software, K.M. and F.P. (Francesco Pierotti); validation, F.P. (Francesco Pierotti), K.M., G.P. and F.T.; formal analysis, K.M. and S.O.; investigation, K.M., F.P. (Francesca Pulvirenti), L.D., M.B., G.P., F.P. (Francesco Pierotti) and F.T.; resources, L.C., A.C. and S.O.; data curation, K.M. and F.P. (Francesco Pierotti); writing—original draft preparation, K.M.; writing—review and editing, K.M., F.P. (Francesca Pulvirenti), F.P. (Francesco Pierotti), L.D., M.B., G.P., F.T., L.T., S.T., L.C., A.C., S.O. and S.M.; visualization, K.M.; supervision, L.C., S.M., A.C. and S.O.; project administration, A.C. and S.O.; funding acquisition, A.C. and S.O. All authors have read and agreed to the published version of the manuscript.

**Funding:** This work was supported by the PRIN 2022 project titled "VR-BCI4PM: A virtual reality system controlled by a hybrid brain–computer interface to improve powered mobility in individuals with neuromotor disorders" (Project Code: 2022BCZ52A_001, CUP: J53D23000690006), funded under the National Recovery and Resilience Plan (PNRR)–Mission 4–Component 2–Investment 1.1 "Fund for the National Research Program and Projects of Significant National Interest (PRIN)" (Call issued by Ministerial Decree No. 104 of 2 February 2022).

**Institutional Review Board Statement:** The study was conducted in accordance with the ethical principles established by the Declaration of Helsinki and was approved by the local Ethical Committee (37-2023-OSS-AUSLBO) on 27 January 2023. The protocol is registered on ClinicalTrials.gov (ID: NCT06586125).

**Informed Consent Statement:** Informed consent was obtained from all subjects involved in the study.

**Data Availability Statement:** The data presented in this study are available on request from the corresponding author. The data are not publicly available due to privacy and ethical reasons.

**Acknowledgments:** The authors would like to express their deepest gratitude to the children, adolescents, and their families who participated in this study. Their time, patience, and engagement were essential to the success of this research. During the preparation of this manuscript, the authors used Google Gemini (https://gemini.google.com) for the purposes of language editing and structural formatting assistance. The authors have reviewed and edited the output and take full responsibility for the content of this publication.

**Conflicts of Interest:** The authors declare no conflicts of interest.

## Abbreviations

The following abbreviations are used in this manuscript:

| | |
|---|---|
| BCIs | Brain–Computer Interfaces |
| CAR | Common Average Reference |
| CP | Cerebral Palsy |
| EEG | Electroencephalography |
| EF–E | Elbow Flexion–Extension |
| EOG | Electrooculography |
| F | Female |
| FI | Fully Immersive |
| FN | False Negative |
| FP | False Positive |
| GMFCS | Gross Motor Function Classification System |
| HanOC | Hand Opening–Closing |
| HMDs | Head-Mounted Displays |
| ID | Identifier |
| IF F–E | Index Finger Flexion–Extension |
| IRCCS-ISNB | IRCCS Institute of Neurological Sciences of Bologna |
| KMI | Kinesthetic Motor Imagery |
| KMIT | KMI Training |
| LL | Lower Limbs |
| M | Male |
| MI | Motor Imagery |
| MSAQ | Motion Sickness Assessment Questionnaire |
| NASA-TLX | NASA Task Load Index |
| PE | Post Evaluation |
| PM | Powered Mobility |
| PMP | Powered Mobility Program |
| PN | Post Navigation |
| PS | Pre Session |
| PW | Powered Wheelchairs |
| SD | Standard Deviation |
| SI | Semi-Immersive |
| SMA II | Spinal Muscular Atrophy Type II |
| SSQ | Simulator Sickness Questionnaire |
| SSVEPs | Steady-State Visual Evoked Potentials |
| TN | True Negative |
| TP | True Positive |
| UL | Upper Limb |
| UOC-MRI | UOC Medicina Riabilitativa Infantile |
| VR | Virtual Reality |
| WISC-IV | Wechsler Intelligence Scale for Children–Fourth Edition |
| WPPSI-III | Wechsler Preschool and Primary Scale of Intelligence–Third Edition |
| WT | Wheelchair Training |

## References


1. Bottos, M.; Bolcati, C.; Sciuto, L.; Ruggeri, C.; Feliciangeli, A. Powered wheelchairs and independence in young children with tetraplegia. *Dev. Med. Child. Neurol.* **2001**, *43*, 769–777. [CrossRef]
2. World Health Organization (WHO). WHO Disability 2023. Available online: https://www.who.int/news-room/fact-sheets/detail/disability-and-health (accessed on 4 February 2025).
3. Fehr, L.; Langbein, W.E.; Skaar, S.B. Adequacy of power wheelchair control interfaces for persons with severe disabilities: A clinical survey. *J. Rehabil. Res. Dev.* **2000**, *37*, 353–360.
4. Simpson, R. Smart wheelchairs: A literature review. *J. Rehabil. Res. Dev.* **2005**, *42*, 423–436. [CrossRef]
5. Domingues, I.; Pinheiro, J.; Silveira, J.; Francisco, P.; Jutai, J.; Correia Martins, A. Psychosocial Impact of Powered Wheelchair, Users' Satisfaction and Their Relation to Social Participation. *Technologies* **2019**, *7*, 73. [CrossRef]
6. Furumasu, J.; Guerette, P.; Tefft, D. The development of a powered wheelchair mobility program for young children. *Technol. Disabil.* **1996**, *5*, 41–48. [CrossRef]
7. Lam, J.-F.; Gosselin, L.; Rushton, P.W. Use of Virtual Technology as an Intervention for Wheelchair Skills Training: A Systematic Review. *Arch. Phys. Med. Rehabil.* **2018**, *99*, 2313–2341. [CrossRef]
8. Abich, J.; Parker, J.; Murphy, J.S.; Eudy, M. A review of the evidence for training effectiveness with virtual reality technology. *Virtual Real.* **2021**, *25*, 919–933. [CrossRef]
9. Gefen, N.; Archambault, P.S.; Rigbi, A.; Weiss, P.L. Pediatric powered mobility training: Powered wheelchair versus simulator-based practice. *Assist. Technol.* **2023**, *35*, 389–398. [CrossRef]
10. de Sá, A.A.R.; Morère, Y.; Naves, E.L.M. Skills assessment metrics of electric powered wheelchair driving in a virtual environment: A survey. *Med. Biol. Eng. Comput.* **2022**, *60*, 323–335. [CrossRef]
11. Abellard, P.; Randria, I.; Abellard, A.; Khelifa, M.M.; Ramanantsizehena, P. Electric Wheelchair Navigation Simulators: Why, when, how? In *Mechatronic Systems Applications*; IntechOpen: London, UK, 2010. [CrossRef]
12. Tao, G.; Archambault, P.S. Powered wheelchair simulator development: Implementing combined navigation-reaching tasks with a 3D hand motion controller. *J. Neuroeng. Rehabil.* **2016**, *13*, 3. [CrossRef]
13. Wen, D.; Liang, B.; Zhou, Y.; Chen, H.; Jung, T.-P. The Current Research of Combining Multi-Modal Brain-Computer Interfaces With Virtual Reality. *IEEE J. Biomed. Health Inform.* **2021**, *25*, 3278–3287. [CrossRef]
14. Belwafi, K.; Ghaffari, F. Thought-Controlled Computer Applications: A Brain–Computer Interface System for Severe Disability Support. *Sensors* **2024**, *24*, 6759. [CrossRef]
15. Jamil, N.; Belkacem, A.N.; Ouhbi, S.; Lakas, A. Noninvasive Electroencephalography Equipment for Assistive, Adaptive, and Rehabilitative Brain-Computer Interfaces: A Systematic Literature Review. *Sensors* **2021**, *21*, 4754. [CrossRef]
16. Lécuyer, A.; Lotte, F.; Reilly, R.B.; Leeb, R.; Hirose, M.; Slater, M. Brain-Computer Interfaces, Virtual Reality, and Videogames. *Computer* **2008**, *41*, 66–72. [CrossRef]
17. Chaudhary, U.; Birbaumer, N.; Ramos-Murguialday, A. Brain-computer interfaces for communication and rehabilitation. *Nat. Rev. Neurol.* **2016**, *12*, 513–525. Correction in *Nat. Rev. Neurol.* **2017**, *13*, 191. [CrossRef]
18. Bobier, C.A.; Peyravi, R.; Hurst, D. Small Brains, Big Data: The Current Landscape of Pediatric Brain-Computer Interface Clinical Trials. *J. Child Neurol.* **2026**, 08830738261467621. [CrossRef]
19. Orlandi, S.; House, S.C.; Karlsson, P.; Saab, R.; Chau, T. Brain-Computer Interfaces for Children with Complex Communication Needs and Limited Mobility: A Systematic Review. *Front. Hum. Neurosci.* **2021**, *15*, 643294. [CrossRef]
20. Mussi, M.G.; Adams, K.D. EEG hybrid brain-computer interfaces: A scoping review applying an existing hybrid-BCI taxonomy and considerations for pediatric applications. *Front. Hum. Neurosci.* **2022**, *16*, 1007136. [CrossRef]
21. Niu, X.; Yuan, M.; Wang, D. Influence of age, cognitive function, attention, and mental state on the effectiveness of EEG-based brain-computer interface device use: A systematic review. *J. Neuroeng. Rehabil.* **2025**, *22*, 270. [CrossRef]
22. Floreani, E.D.; Rowley, D.; Kelly, D.; Kinney-Lang, E.; Kirton, A. On the feasibility of simple brain-computer interface systems for enabling children with severe physical disabilities to explore independent movement. *Front. Hum. Neurosci.* **2022**, *16*, 1007199. [CrossRef]
23. Jadavji, Z.; Zewdie, E.; Kelly, D.; Kinney-Lang, E.; Robu, I.; Kirton, A. Establishing a Clinical Brain-Computer Interface Program for Children with Severe Neurological Disabilities. *Cureus* **2022**, *14*, e26215. [CrossRef]
24. Pfurtscheller, G.; Lopes da Silva, F.H. Event-related EEG/MEG synchronization and desynchronization: Basic principles. *Clin. Neurophysiol.* **1999**, *110*, 1842–1857. [CrossRef] [PubMed]
25. Wolpaw, J.; Wolpaw, E.W. (Eds.) *Brain–Computer Interfaces: Principles and Practice*; Oxford University Press: Oxford, UK, 2012. [CrossRef]
26. Reyhani-Masoleh, B.; Chau, T. Navigating in Virtual Reality using Thought: The Development and Assessment of a Motor Imagery based Brain-Computer Interface. *arXiv* **2019**, arXiv:1912.04828. [CrossRef]

27. Stinear, C.M.; Byblow, W.D.; Steyvers, M.; Levin, O.; Swinnen, S.P. Kinesthetic, but not visual, motor imagery modulates corticomotor excitability. *Exp. Brain Res.* **2006**, *168*, 157–164. [CrossRef]
28. Toriyama, H.; Ushiba, J.; Ushiyama, J. Subjective Vividness of Kinesthetic Motor Imagery Is Associated with the Similarity in Magnitude of Sensorimotor Event-Related Desynchronization Between Motor Execution and Motor Imagery. *Front. Hum. Neurosci.* **2018**, *12*, 295. [CrossRef]
29. Keough, J.R.; Irvine, B.; Kelly, D.; Wrightson, J.; Comaduran Marquez, D.; Kinney-Lang, E.; Kirton, A. Fatigue in children using motor imagery and P300 brain-computer interfaces. *J. Neuroeng. Rehabil.* **2024**, *21*, 61. [CrossRef]
30. Kinney-Lang, E.; Auyeung, B.; Escudero, J. Expanding the (kaleido)scope: Exploring current literature trends for translating electroencephalography (EEG) based brain–computer interfaces for motor rehabilitation in children. *J. Neural Eng.* **2016**, *13*, 061002. [CrossRef]
31. Filho, C.A.S.; Serrano, J.I.; Attux, R.; Castellano, G.; Rocon, E.; del Castillo, M.D. Reorganization of Resting-State EEG Functional Connectivity Patterns in Children with Cerebral Palsy Following a Motor Imagery Virtual-Reality Intervention. *Appl. Sci.* **2021**, *11*, 2372. [CrossRef]
32. Gentile, A.E.; Rinella, S.; Desogus, E.; Verrelli, C.M.; Iosa, M.; Perciavalle, V.; Ruggieri, M.; Polizzi, A. Motor imagery for paediatric neurorehabilitation: How much do we know? Perspectives from a systematic review. *Front. Hum. Neurosci.* **2024**, *18*, 1245707. [CrossRef]
33. Holmes, C.J.; MacDonald, H.V.; Esco, M.R.; Fedewa, M.V.; Wind, S.A.; Winchester, L.J. Comparison of Heart Rate Variability Responses to Varying Resistance Exercise Volume-Loads. *Res. Q. Exerc. Sport* **2022**, *93*, 391–400. [CrossRef]
34. Tiwari, R.; Kumar, R.; Malik, S.; Raj, T.; Kumar, P. Analysis of Heart Rate Variability and Implication of Different Factors on Heart Rate Variability. *Curr. Cardiol. Rev.* **2021**, *17*, e160721189770. [CrossRef]
35. An, X.; Kuang, D.; Guo, X.; Zhao, Y.; He, L. A Deep Learning Method for Classification of EEG Data Based on Motor Imagery. In *Intelligent Computing in Bioinformatics*; Springer: Cham, Switzerland, 2014.
36. Hammond, L.; Rowley, D.; Tuck, C.; Floreani, E.D.; Wieler, A.; Kim, V.S.-H.; Bahari, H.; Andersen, J.; Kirton, A.; Kinney-Lang, E. BCI move: Exploring pediatric BCI-controlled power mobility. *Front. Hum. Neurosci.* **2025**, *19*, 1456692. [CrossRef]
37. Palisano, R.J.; Rosenbaum, P.; Bartlett, D.; Livingston, M.H. Content validity of the expanded and revised Gross Motor Function Classification System. *Dev. Med. Child. Neurol.* **2008**, *50*, 744–750. [CrossRef]
38. Panachakel, J.T.; Vinayak, N.N.; Nunna, M.; Ramakrishnan, A.G.; Sharma, K. An Improved EEG Acquisition Protocol Facilitates Localized Neural Activation. In *Advances in Communication Systems and Networks*; Springer: Singapore, 2020.
39. Tonin, L.; Beraldo, G.; Tortora, S.; Menegatti, E. ROS-Neuro: An Open-Source Platform for Neurorobotics. *Front. Neurorobot* **2022**, *16*, 886050. [CrossRef]
40. Marcaccini, K.; Pulvirenti, F.R.; Pierotti, F.; Arcobelli, V.A.; Tonin, L.; Tortora, S.; Groppi, A.; Giorgi, F.; Dellarole, L.; Chiari, L.; et al. Toward Inclusive Powered Mobility: A Novel Protocol Utilizing a Hybrid EOG-EEG BCI in a VR-Based Wheelchair Driving Simulator. In Proceedings of the 2025 IEEE International Conference on Systems, Man, and Cybernetics (SMC), Vienna, Austria, 5–8 October, 2025; pp. 4572–4578. [CrossRef]
41. Mazloumi Gavgani, A.; Walker, F.R.; Hodgson, D.M.; Nalivaiko, E. A comparative study of cybersickness during exposure to virtual reality and "classic" motion sickness: Are they different? *J. Appl. Physiol.* **2018**, *125*, 1670–1680. [CrossRef]
42. Kaimara, P.; Oikonomou, A.; Deliyannis, I. Could virtual reality applications pose real risks to children and adolescents? A systematic review of ethical issues and concerns. *Virtual Real.* **2022**, *26*, 697–735. [CrossRef]
43. Bexson, C.; Oldham, G.; Wray, J. Safety of virtual reality use in children: A systematic review. *Eur. J. Pediatr.* **2024**, *183*, 2071–2090. [CrossRef]
44. Gianaros, P.J.; Muth, E.R.; Mordkoff, J.T.; Levine, M.E.; Stern, R.M. A questionnaire for the assessment of the multiple dimensions of motion sickness. *Aviat. Space Environ. Med.* **2001**, *72*, 115–119.
45. Kennedy, R.S.; Lane, N.E.; Berbaum, K.S.; Lilienthal, M.G. Simulator Sickness Questionnaire: An Enhanced Method for Quantifying Simulator Sickness. *Int. J. Aviat. Psychol.* **1993**, *3*, 203–220. [CrossRef] [PubMed]
46. Salimi, Z.; Ferguson-Pell, M.W. Motion sickness and sense of presence in a virtual reality environment developed for manual wheelchair users, with three different approaches. *PLoS ONE* **2021**, *16*, e0255898. [CrossRef]
47. Goble, M.S.L.; Raison, N.; Mekhaimar, A.; Dasgupta, P.; Ahmed, K. Adapting Motor Imagery Training Protocols to Surgical Education: A Systematic Review and Meta-Analysis. *Surg. Innov.* **2021**, *28*, 329–351. [CrossRef]
48. Hilt, P.M.; Bertrand, M.F.; Féasson, L.; Lebon, F.; Mourey, F.; Ruffino, C.; Rozand, V. Motor Imagery Training Is Beneficial for Motor Memory of Upper and Lower Limb Tasks in Very Old Adults. *Int. J. Environ. Res. Public Health* **2023**, *20*, 3541. [CrossRef]
49. Rozand, V.; Lebon, F.; Stapley, P.J.; Papaxanthis, C.; Lepers, R. A prolonged motor imagery session alter imagined and actual movement durations: Potential implications for neurorehabilitation. *Behav. Brain Res.* **2016**, *297*, 67–75. [CrossRef]

50. Tonin, L.; Bauer, F.C.; Millán, J.d.R. The Role of the Control Framework for Continuous Teleoperation of a Brain–Machine Interface-Driven Mobile Robot. *IEEE Trans. Robot.* **2020**, *36*, 78–91. [CrossRef]
51. Hart, S.G.; Staveland, L.E. Development of NASA-TLX (Task Load Index): Results of Empirical and Theoretical Research. In *Human Mental Workload*; Hancock, P.A., Meshkati, N., Eds.; North-Holland: Amsterdam, The Netherlands, 1988; Volume 52, pp. 139–183. [CrossRef]
52. Guger, C.; Edlinger, G.; Harkam, W.; Niedermayer, I.; Pfurtscheller, G. How many people are able to operate an EEG-based brain-computer interface (BCI)? *IEEE Trans. Neural Syst. Rehabil. Eng.* **2003**, *11*, 145–147. [CrossRef]
53. Cincotti, F.; Mattia, D.; Aloise, F.; Bufalari, S.; Schalk, G.; Oriolo, G.; Cherubini, A.; Marciani, M.G.; Babiloni, F. Non-invasive brain–computer interface system: Towards its application as assistive technology. *Brain Res. Bull.* **2008**, *75*, 796–803. [CrossRef]
54. Tiwari, S.; Goel, S.; Bhardwaj, A. MIDNN- a classification approach for the EEG based motor imagery tasks using deep neural network. *Appl. Intell.* **2022**, *52*, 4824–4843. [CrossRef]
55. Ghritlahare, R.; Sahu, M.; Kumar, R. Classification of Two-Class Motor Imagery EEG Signals Using Empirical Mode Decomposition and Hilbert–Huang Transformation. In *Computing and Network Sustainability*; Peng, S.-L., Dey, N., Bundele, M., Eds.; Springer: Singapore, 2019; pp. 375–386.
56. Kauati-Saito, E.; Pereira, A.D.; Fontana, A.P.; de Sá, A.M.; Soares, J.G.; Tierra-Criollo, C.J. Classification of Different Motor Imagery Tasks with the Same Limb Using Electroencephalographic Signals. *Sensors* **2025**, *25*, 5291. [CrossRef]
57. Pfurtscheller, G.; Linortner, P.; Winkler, R.; Korisek, G.; Müller-Putz, G. Discrimination of Motor Imagery-Induced EEG Patterns in Patients with Complete Spinal Cord Injury. *Comput. Intell. Neurosci.* **2009**, *2009*, 104180. [CrossRef]
58. Donchin, E.; Spencer, K.M.; Wijesinghe, R. The mental prosthesis: Assessing the speed of a P300-based brain-computer interface. *IEEE Trans. Rehabil. Eng.* **2000**, *8*, 174–179. [CrossRef] [PubMed]
59. Fierro-Marrero, J.; Corujo-Merino, A.; La Touche, R.; Lerma-Lara, S. Motor imagery ability in children and adolescents with cerebral palsy: A systematic review and evidence map. *Front. Neurol.* **2024**, *15*, 1325548. [CrossRef]
60. Shin, Y.K.; Lee, D.R.; Hwang, H.J.; You, S.J.H.; Im, C.H. A novel EEG-based brain mapping to determine cortical activation patterns in normal children and children with cerebral palsy during motor imagery tasks. *NeuroRehabilitation* **2012**, *31*, 349–355. [CrossRef]
61. Daly, I.; Billinger, M.; Laparra-Hernández, J.; Aloise, F.; García, M.L.; Faller, J.; Scherer, R.; Müller-Putz, G. On the control of brain-computer interfaces by users with cerebral palsy. *Clin. Neurophysiol.* **2013**, *124*, 1787–1797. [CrossRef]
62. Georgiadis, K.; Laskaris, N.; Nikolopoulos, S.; Kompatsiaris, I. Exploiting the heightened phase synchrony in patients with neuromuscular disease for the establishment of efficient motor imagery BCIs. *J. Neuroeng. Rehabil.* **2018**, *15*, 90. [CrossRef]
63. Hashimoto, Y.; Ushiba, J.; Kimura, A.; Liu, M.; Tomita, Y. Change in brain activity through virtual reality-based brain-machine communication in a chronic tetraplegic subject with muscular dystrophy. *BMC Neurosci.* **2010**, *11*, 117. [CrossRef]
64. Bora-Zereyak, M.; Bulut, N.; Yılmaz, Ö.; Alemdaroğlu-Gürbüz, İ. Motor imagery ability of children with duchenne muscular dystrophy: Reliability and validity of kinesthetic and Visual Imagery Questionnaire-10, and its association with cognitive status. *Eur. J. Paediatr. Neurol.* **2024**, *51*, 118–124. [CrossRef]
65. Ma, J.; Yang, B.; Qiu, W.; Li, Y.; Gao, S.; Xia, X. A large EEG dataset for studying cross-session variability in motor imagery brain-computer interface. *Sci. Data* **2022**, *9*, 531. [CrossRef]
66. Ramu, V.; Lakshminarayanan, K. Enhanced motor imagery of digits within the same hand via vibrotactile stimulation. *Front. Neurosci.* **2023**, *17*, 1152563. [CrossRef]
67. Pfurtscheller, G.; Neuper, C. Motor imagery and direct brain-computer communication. *Proc. IEEE* **2001**, *89*, 1123–1134. [CrossRef]
68. Khanna, P.; Carmena, J.M. Beta band oscillations in motor cortex reflect neural population signals that delay movement onset. *eLife* **2017**, *6*, e24573. [CrossRef]
69. Lin, Q.; Zhang, Y.; Zhang, Y.; Zhuang, W.; Zhao, B.; Ke, X.; Peng, T.; You, T.; Jiang, Y.; Yilifate, A.; et al. The Frequency Effect of the Motor Imagery Brain Computer Interface Training on Cortical Response in Healthy Subjects: A Randomized Clinical Trial of Functional Near-Infrared Spectroscopy Study. *Front. Neurosci.* **2022**, *16*, 810553. [CrossRef]
70. Laver, K.E.; Lange, B.; George, S.; Deutsch, J.E.; Saposnik, G.; Crotty, M. Virtual reality for stroke rehabilitation. *Cochrane Database Syst. Rev.* **2017**, *11*, CD008349. [CrossRef] [PubMed]
71. Tonin, L.; Millán, J.D.R. Noninvasive Brain–Machine Interfaces for Robotic Devices. *Annu. Rev. Control Robot. Auton. Syst.* **2021**, *4*, 191–214. [CrossRef]
72. Tonin, L.; Perdikis, S.; Kuzu, T.D.; Pardo, J.; Orset, B.; Lee, K.; Aach, M.; Schildhauer, T.A.; Martínez-Olivera, R.; Millán, J.d.R. Learning to control a BMI-driven wheelchair for people with severe tetraplegia. *iScience* **2022**, *25*, 105418. [CrossRef]
73. Carlson, T.; Monnard, G.; Millán, J.D.R.; Millan, R. Vision-Based Shared Control for a BCI Wheelchair. *Int. J. Bioelectromagn.* **2011**, *13*, 20–21.

74. Glavas, K.; Tzimourta, K.; Tzallas, A.; Giannakeas, N.; Tsipouras, M. Empowering Individuals with Disabilities: A 4-DoF BCI Wheelchair Using MI and EOG Signals. *IEEE Access* **2024**, *12*, 95417–95433. [CrossRef]
75. Bobier, C.; Hurst, D.J. Implanted Pediatric Brain-Computer Interface Research: Recommendations for the Ethical Design of Clinical Trials. *AJOB Neurosci*. **2026**, 1–12. [CrossRef]

**Disclaimer/Publisher's Note:** The statements, opinions and data contained in all publications are solely those of the individual author(s) and contributor(s) and not of MDPI and/or the editor(s). MDPI and/or the editor(s) disclaim responsibility for any injury to people or property resulting from any ideas, methods, instructions or products referred to in the content.